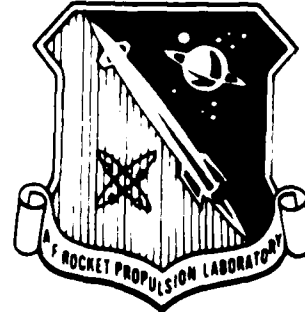LEVEL

AFRPL-TR-81-52

AD A104746

PREFRACTURE BEHAVIOR OF SOLID PROPELLANTS

C. C. Hsiao

S. S. Chern

C. H. Cheng

Department of Aerospace Engineering and Mechanics
University of Minnesota
Minneapolis, Minnesota 55455

JULY 1981

Final Report for Period September 1978 - July 1980

Approved for Public Release; Distribution Unlimited

DTIC
S ELECTED
SEP 29 1981
F

Prepared for

AIR FORCE ROCKET PROPULSION LABORATORY
DIRECTOR OF SCIENCE AND TECHNOLOGY
AIR FORCE SYSTEMS COMMAND
EDWARDS AFB, CALIFORNIA 93523

DTIC FILE COPY

NOTICES

When U.S. Government drawings, specifications, or other data are used for any purpose other than a definitely related Government procurement operation, the fact that the Government may have formulated, furnished, or in any way supplied the said drawings, specifications, or other data, is not to be regarded by implication or otherwise, or in any manner licensing the holder or any other person or corporation, or conveying any rights or permission to manufacture, use, or sell any patented invention that may be related thereto.

FOREWORD

This report was submitted by the Department of Aerospace Engineering and Mechanics of the University of Minnesota, 2642 University Avenue, St Paul, Minnesota 55114, under Contract F04611-78-C-0078, Job Order No. 573013DJ with the Air Force Rocket Propulsion Laboratory, Edwards AFB, CA 93523. The Principal Investigator was Prof C. C. Hsiao. Major contributors were S. S. Chern and C. H. Cheng.

DURWOOD I. THRASHER
Project Manager

R. JOHN MOSS, Capt, USAF
Ch, Mechanical Behavior and
Aging Section

FOR THE COMMANDER

CHARLES R. COOKE
Director, Solid Rocket Division

REPORT DOCUMENTATION PAGE		READ INSTRUCTIONS BEFORE COMPLETING FORM
1. REPORT NUMBER AFRPL-TR-81-52	2. GOVT ACCESSION NO. AD-A204 746	3. RECIPIENT'S CATALOG NUMBER
4. TITLE *(and Subtitle)* PREFRACTURE BEHAVIOR OF SOLID PROPELLANTS		5. TYPE OF REPORT & PERIOD COVERED Final Rept. September 1978- July 1980
		6. PERFORMING ORG. REPORT NUMBER
7. AUTHOR(s) C. C. Hsiao C. H. Cheng S. S. Chern		8. CONTRACT OR GRANT NUMBER(s) F04611-78-C-0078
9. PERFORMING ORGANIZATION NAME AND ADDRESS Dept of Aerospace Engineering and Mechanics University of Minnesota Minneapolis, Minnesota 55455		10. PROGRAM ELEMENT, PROJECT, TASK AREA & WORK UNIT NUMBERS 61102F Project 2307, Task M1 2307M1DJ
11. CONTROLLING OFFICE NAME AND ADDRESS AF Rocket Propulsion Laboratory/MKPB Edwards AFB, CA 93523		12. REPORT DATE July 1981
		13. NUMBER OF PAGES 72
14. MONITORING AGENCY NAME & ADDRESS*(If different from Controlling Office)*		15. SECURITY CLASS. *(of this report)* Unclassified
		15a. DECLASSIFICATION/DOWNGRADING SCHEDULE

16. DISTRIBUTION STATEMENT *(of this Report)*

Approved for Public Release; Distribution unlimited.

17. DISTRIBUTION STATEMENT *(of the abstract entered in Block 20, if different from Report)*

18. SUPPLEMENTARY NOTES

19. KEY WORDS *(Continue on reverse side if necessary and identify by block number)*

Prefracture Behavior   Laser Speckle Interferometry
Solid Propellants
Crazing
Fracture
Filled Polymers

20. ABSTRACT *(Continue on reverse side if necessary and identify by block number)*

An experimental and theoretical study of prefracture behavior of solid propellant polymer is presented. A one-dimensional mathematical model for a two-dimensional craze is developed and compared with measured results.

DD FORM 1 JAN 73 **1473**   EDITION OF 1 NOV 65 IS OBSOLETE

TABLE OF CONTENTS

TABLE OF CONTENTS

LIST OF ILLUSTRATIONS

LIST OF ILLUSTRATIONS

LIST OF TABLES

1. BACKGROUND AND INTRODUCTION

The initiation and propagagtion of macro-fractures in solid propellant rocket motor grains is a frequent structural problem. Much exploratory development effort has been conducted in attempting to obtain reliable predictive measures for solid propellant fracture with only limited success. One factor involved in this situation is the inadequate understanding of the physical processes which occur in propellants under stress prior to the appearance of fracture surfaces. Research into propellant prefracture behavior should provide a better understanding and foundation for future development of fracture prediction methods.

A preliminary research in propellant prefracture behavior has been conducted during the past 23 months. Both theoretical and experimental approaches have been carried out according to three phases of a program.

Phase I was primarily concerned with the development of a mathematical model which would be applicable to a single prefracture configuration of solid propellant under stress. The occurence of such a prefracture configuration in polymeric systems is usually termed a craze. Concurrently an experimental technique was to be developed for determining the displacement and stress fields in the vicinity of a craze. During this phase some specially prepared propellant polymers with and without ammonium perchlorate were tested.

In Phase II extension to highly filled propellant polymer samples was to be added to the investigations. Phase III was to extend the studies to massive crazing and craze-crack transitition and fracture propagation.

This report covers the attempts made and work done in Phase I. Since the nature of this research is basic and complex, the efforts and developments are reported under separate headings as reflected in Section 2.

2. DEVELOPMENT AND APPLICATION OF THEORIES

In order to develop an effective mathematical model for analyzing prefracture behavior of solid propellants under stress, several approaches have been considered. A two-dimensional formulation of a single craze in

propellant polymer, an improved double beam model for large deformations and the time dependent behavior of craze propagation have all been attempted. These together with the development of a laser speckle technique for displacement measurement are reported separately in the following subsections.

2.1 Prefracture Analysis of 2D Craze in Propellant Polymers

2.1.1 Introduction

Under tensile stresses certain high polymers deform from sites where stress concentrations are created and crazes develop. The development of crazing in polymers is a prefracture phenomenon. The mechanism of the development of a single craze is complex. After the nucleation of a craze to the naked eye it appears like a crack. Thus the analysis of a crack has been utilized to study the craze. Since there is no material present within the crack, but a new phase of oriented polymeric molecules fill in a craze which act as boundary stresses, any governing formulations should at least include this feature for adequate analysis. This report limits its scope to consider such an approach.

2.1.2 2D Craze Formulation

As shown in Figure 1, a two-dimensional craze is considered to occur in an infinite sheet in a simple tension stress field with magnitude σ_o vertically in a rectangular coordinate system $Oxyz$. A craze is assumed to have developed horizontally along the x coordinate with oriented polymer molecule strands acting as prescribed craze boundary stresses in the z-direction.

Using linear elasticity theory, if the body forces are neglected, the two-dimensional biharmonic equation

$$\nabla^2 \nabla^2 \phi = 0, \tag{1}$$

where ϕ is a stress function, governs the state of stress of a plane problem such that the stress components are given by

$$\sigma_{xx} = \partial^2 \phi / \partial z^2, \tag{2}$$

$$\sigma_{zz} = \partial^2 \phi / \partial x^2, \tag{3}$$

and $\sigma_{xz} = -\partial^2 \phi / \partial x \partial z. \tag{4}$
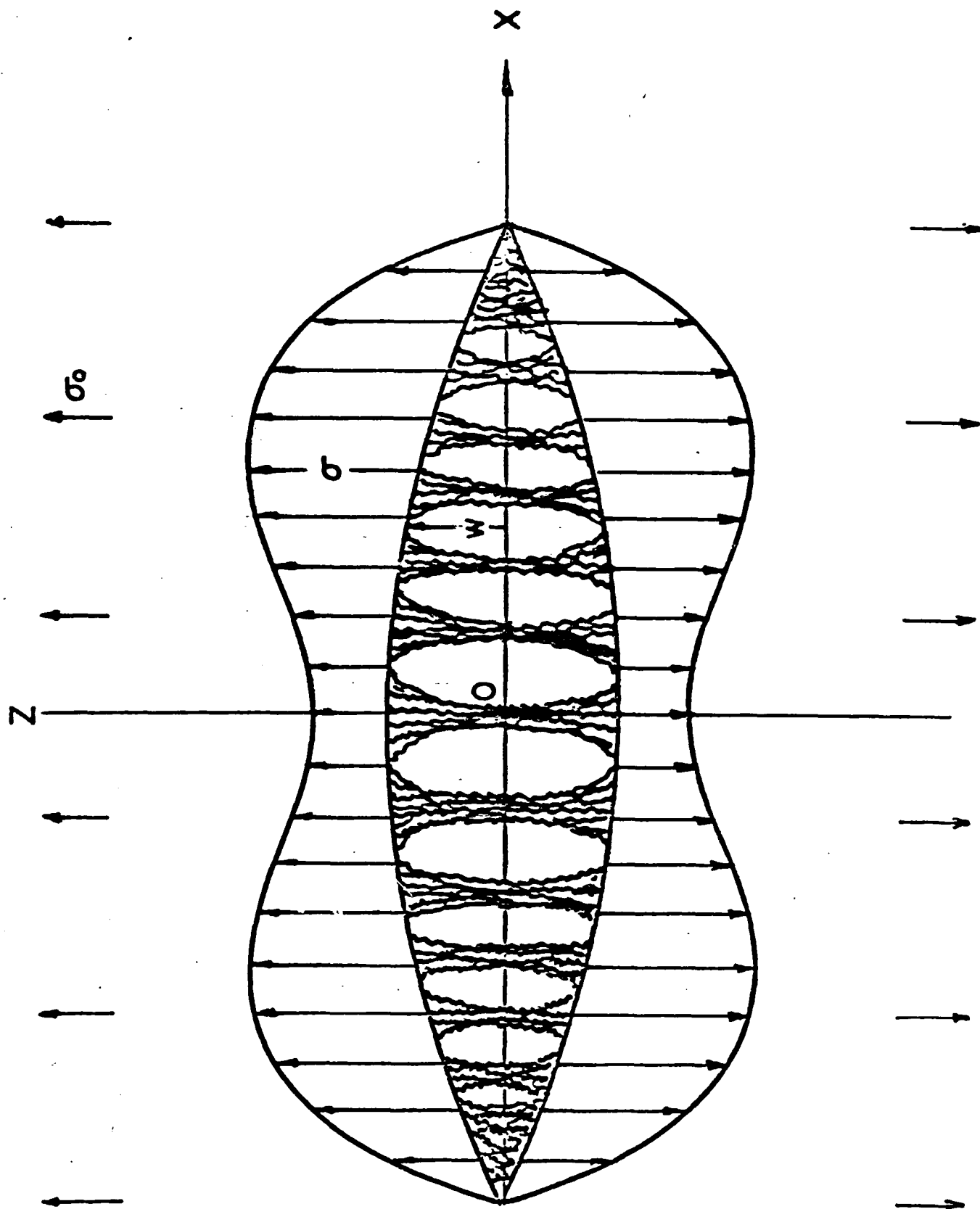
Figure 1.   Schematic Diagram of Craze Displacement and Stress Distribution in Polymer Surface

7

The mathematical description of this boundary value problem is to find Φ such that Equation 1 is satisfied, however, subject to the boundary conditions that

$$\sigma_{zz} = \sigma_o, \quad \sigma_{xx} = \sigma_{xz} = 0 \qquad \text{as } (x^2 + z^2)^{\frac{1}{2}} \to \infty \qquad (5)$$

and $\quad \sigma_{zz} = k(x)w(x) \qquad\qquad |x| < c \qquad (6)$

where $k(x)$ is a modulus function, $w(x)$ is the vertical displacement field, and c is the half length of the craze.

The solution of Equation 1 with the above boundary conditions can be obtained using the Fourier transform method:

$$\sigma_{zz}(x) = \sigma_o - (2/\pi) \int_0^\infty \tilde{F}(\xi) \cos(\xi x) d\xi, \qquad (7)$$

$$w(x) = [4(1-\nu^2)/\pi E] \int_0^\infty [\tilde{F}(\xi)/\xi] \cos(\xi x) d\xi, \qquad |x| < c \qquad (8)$$

and $\quad w(x) = 0, \qquad\qquad |x| \geq c \qquad (9)$

where E = modulus of elasticity of the medium,

$\quad \nu$ = Poisson's ratio of the medium,

and $\bar{F}(\xi)$ satisfies the dual integral equations:

$$(2/\pi) \int_0^\infty \tilde{F}(\xi) \cos(\xi x) d\xi = \sigma_o - k(x)w(x), \qquad |x| < c \qquad (10)$$

and $\quad \int_0^\infty [\tilde{F}(\xi)/\xi] \cos(\xi x) d\xi = 0, \qquad |x| \geq c \qquad (11)$

Using dimensionless quantities and solving, eventually

$$\sigma_{zz}(x) = k(x)w(x), \qquad |x| \leq 1 \qquad (12)$$

and $\quad \sigma_{zz}(x) = \dfrac{\sigma_o x}{(x^2-1)^{1/2}} + \dfrac{2}{\pi} \dfrac{d}{dx} \int_0^1 \dfrac{\zeta}{(x^2-\zeta^2)^{1/2}} \int_0^\zeta \dfrac{k(\eta)w(\eta)}{(\zeta^2-\eta^2)^{1/2}} d\eta d\zeta,$

$$|x| \geq 1 \qquad (13)$$

8

where $k(x)$ and $w(x)$ may be in series form and computer programming can be employed to obtain the displacement and stress fields once $k(x)$ is given.

The function used for $k(x)$ is of the following form:

$$k(x) = k_o[f+(1-f)(e^{\lambda x}+e^{-\lambda x}-2)/(e^{\lambda c}+e^{-\lambda c}-2)] \qquad (14)$$

where k_o is a constant modulus of the medium, f is a fraction, and λ is a parameter. Thus for $\lambda = 3$, $f = 0.01$ the modulus function becomes

$$k(x) = k_o[0.010 + 0.491\ x^2 + 0.368\ x^4 + 0.111\ x^6 + 0.018\ x^8$$

$$+ 0.00178\ x^{10} + 0.00012\ x^{12} + ...] \qquad (15)$$

Figures 2 and 3 respectively show the displacement field and the stress field for the modulus function given with $f = 0$, 0.01, 0.1 or 0.5. Dimensionless quantities were used for plotting the results. w/w_o is the dimensionless displacement with w_o as the homogeneous displacement of the medium under the stress σ_o. The dimensionless stress is simply σ/σ_o. The quantity λ was chosen to be 3. For solid propellant polymer, the following data have been used: modulus of elasticity $E = 94.2$ psi, Poisson's ratio $\nu = 0.5$, $\sigma_o = 1$ psi and $k_o = 1000$ psi.

It is estimated that for a common craze of a brittle polymer, f is likely to be around 0.5 or less. When actual fracture develops at the center of a craze, $f = 0$.

2.1.3 <u>Discussion</u> - The analysis is based upon the theory of elasticity for small deformations. Therefore, the results are expected to satisfy the crazing behavior of brittle polymers. For polymeric systems which respond to load in large deformations, this theory is not likely to hold.

2.2 Prefracture Analysis of Craze in Solid Propellant

2.2.1 <u>Introduction</u> - The phenomenon and study of stress crazing in polymeric materials have gained increasing attention and momentum in the recent years. Different models have been suggested to describe the physical and chemical properties of a craze. It has been noticed that the molecular

9
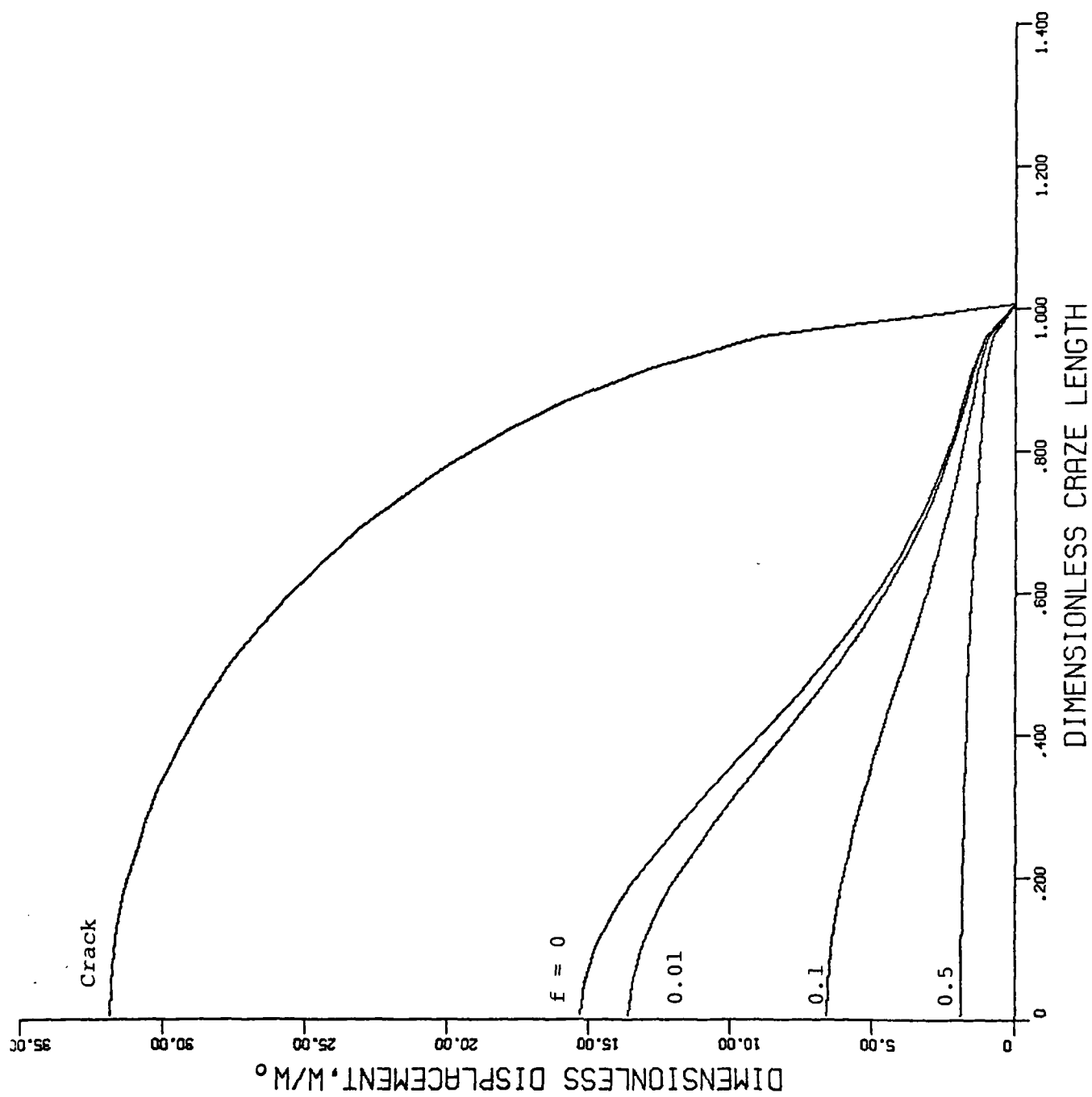
Figure 2. Craze Length vs. Craze Displacement

10
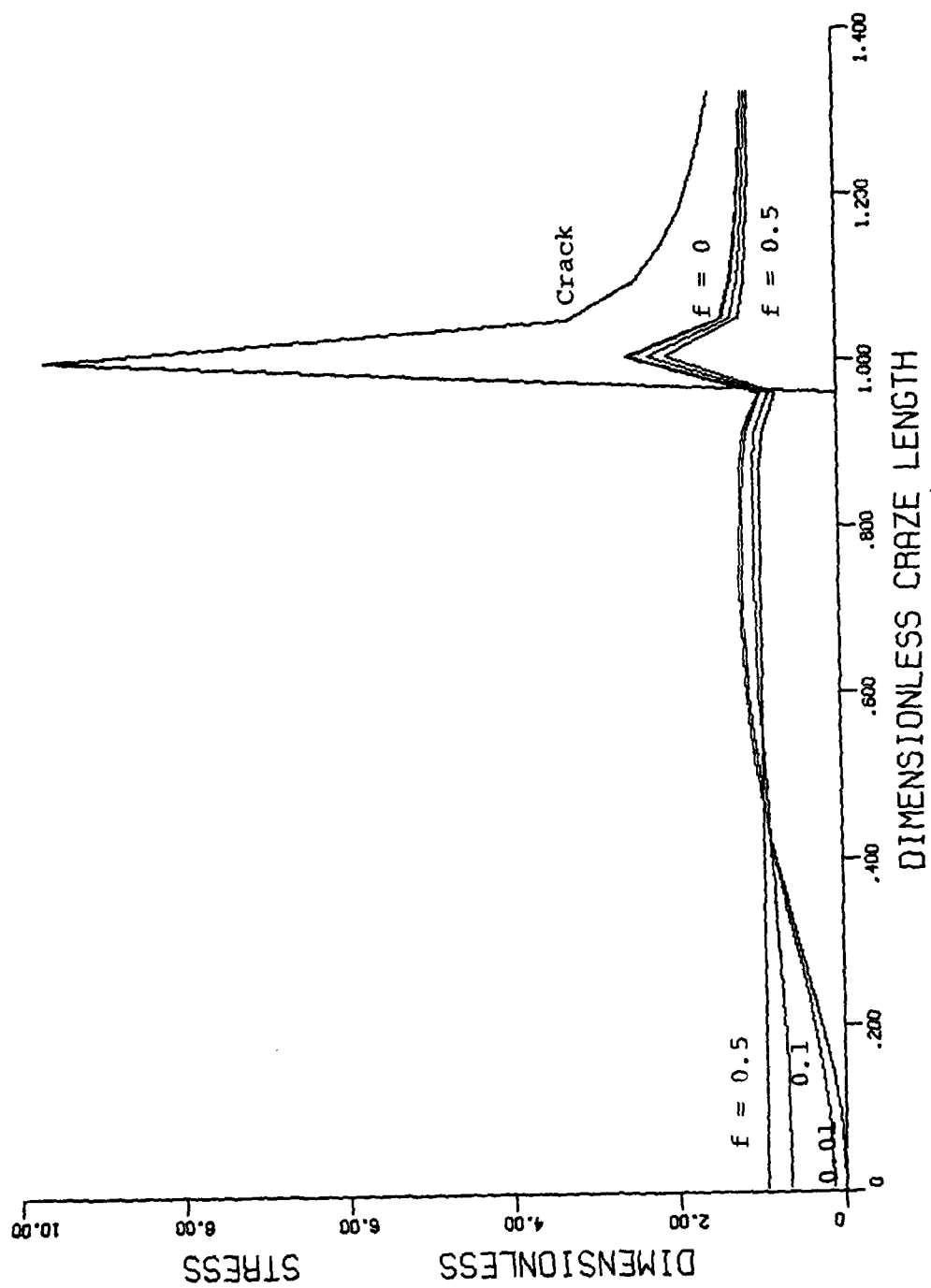
Figure 3. Craze Length vs. Stress Distribution

11

behavior of the partially oriented craze material depends on the stress distribution on the craze boundary which is interrelated to the displacement field of the craze boundary. This report attempts to develop a simple elastic model which can be used to evaluate the craze displacement field directly from a given stress condition. Using the analogy between the contour of a craze boundary and a bar bent to the same contour, the problem can be reduced to a one-dimensional case. As the craze material deforms under geometric constraint, the volume increases while the density decreases and voids and polymer bundles are produced. These oriented polymer bundles behave like elastic springs, and the spring force, together with the tensile stress on the bar, and stress at infinity constitute the force equilibrium on the bar.

2.2.2 <u>Model and Formulation of Governing Equation</u> - Consider an infinite sheet of polymeric material under constant stress σ_o applied at infinity along the z-direction. By placing the cross-section of a craze on the y-z plane as shown in Figure 4 and considering the force balance of an infinitesimal element of the bar, which is subjected to surface tension forces S and S + dS, tensile stress σ_o, *prescribed stress* $\sigma(x)$ and bending stiffness of bar D(x), the displacement field is described by the differential equation

$$D(x)\nabla^2\nabla^2 w(x) - S(x)\nabla^2 w(x) + k(x)w(x) = \sigma_o \qquad (16)$$

where

$w(x)$ = displacement in z-direction,

$D(x)$ = bending stiffness of bar,

$S(x)$ = tensile stress,

and $k(x)w(x) = \sigma(x)$ = prescribed stress due to craze material.

Based on geometry, it has been shown elsewhere that for small displacements, the ratio $k(x)/S(x)$ is constant. And both $E(x)$ and $S(x)$ are properties of the craze bounda⌐ which is made of partially oriented polymeric material and proportional t⌐ the degree of orientation. It is reasonable to assume that $S(x)/D(x)$ is constant. Define

$$\frac{S(x)}{D(x)} \equiv \lambda_1^2 + \lambda_2^2 . \qquad (17)$$

12
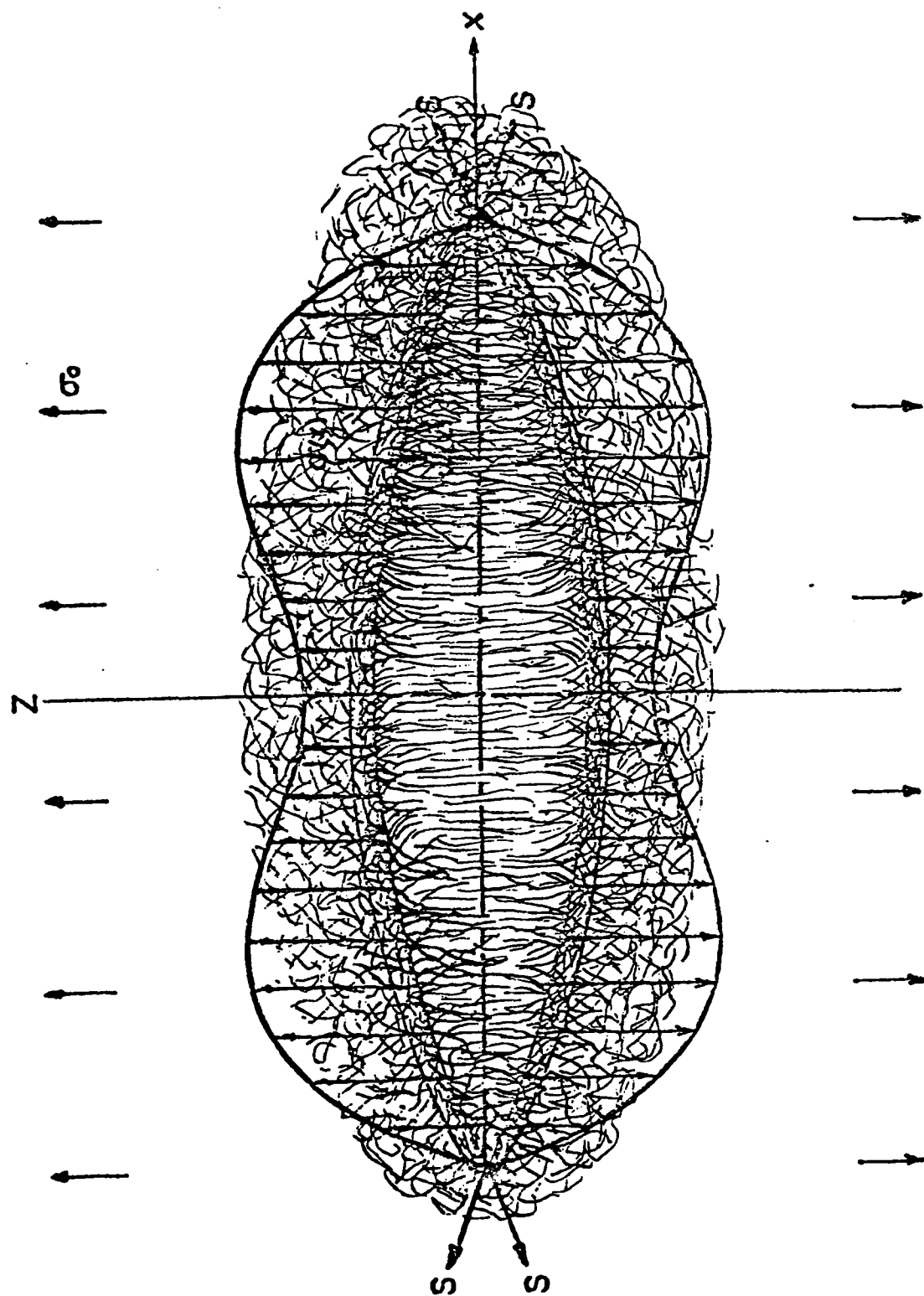
Figure 4. Displacement and stress field at polymer craze boundary.

$$\frac{k(x)}{D(x)} \equiv \lambda_1{}^2 \lambda_2{}^2 , \tag{18}$$

and $\dfrac{\sigma_o}{D(x)} = \dfrac{\sigma_o \lambda_1{}^2 \lambda_2{}^2}{k(x)} \equiv K(x)$ \hfill (19)

where λ_1, λ_2 are constants.

The governing equation becomes:

$$\nabla^2 \nabla^2 w(x) - (\lambda_1{}^2 + \lambda_2{}^2) \nabla^2 w(x) + \lambda_1{}^2 \lambda_2{}^2 w(x) = K(x) . \tag{20}$$

By *symmetry about the z-axis*, it is known that $w(x)$ is an even function. The bar is considered as a cantilever beam built in at the craze tip. This allows room for investigation of stress field beyond the craze tip. In order to be able to obtain solutions in closed form, the following boundary conditions are employed:

$$w'(0) = w''(0) = w(c) = w'(c) = 0 \tag{21}$$

where the primed quantities represent their derivitives with respect to x. Assume the spring constant of the polymer bundles $k(x)$ varies exponentially with x and

$$k(x) = k_o \left[f + (1 - f) \left(\frac{e^{\lambda x} + e^{-\lambda x} - 2}{e^{\lambda c} + e^{-\lambda c} - 2} \right) \right] \tag{22}$$

where

λ is a constant,

k_o is the modulus of elasticity of the bulk material,

and f is a fraction which accounts for the decrease of density of craze material as it deforms.

2.2.3 <u>Solution</u> - General solution of the governing differential equation is

14

$$w(x) = c_1 e^{\lambda_1 x} + c_2 e^{-\lambda_1 x} + c_3 e^{\lambda_2 x} + c_4 e^{-\lambda_2 x}$$

$$+ \int_0^x J(x - \xi) \, K(\xi) \, d\xi \qquad (23)$$

where

$$J(x) \equiv \frac{[\lambda_2 \, (e^{\lambda_1 x} - e^{-\lambda_1 x}) - \lambda_1 (e^{\lambda_2 x} - e^{-\lambda_2 x})]}{2\lambda_1 \lambda_2 \, (\lambda_1^2 - \lambda_2^2)} \, . \qquad (24)$$

Define

$$F(y, \, x) \equiv \int_0^x \frac{e^{y(x - \xi)}}{f(e^{\lambda c} + e^{-\lambda c}) - 2 + (1 - f)(e^{\lambda \xi} + e^{-\lambda \xi})} \, d\xi \, , \qquad (25)$$

then the solution can be written as,

$$w(x) = c_1 e^{\lambda_1 x} + c_2 e^{-\lambda_1 x} + c_3 e^{\lambda_2 x} + c_4 e^{-\lambda_2 x}$$

$$+ \frac{\lambda_1 \lambda_2 \, \sigma_o (e^{\lambda c} + e^{-\lambda c} - 2)}{2k_o (\lambda_1^2 - \lambda_2^2)} \, .$$

$$\cdot [\lambda_2 F(\lambda_1, x) - \lambda_2 F(-\lambda_1, x) - \lambda_1 F(\lambda_2, x) + \lambda_1 F(-\lambda_2, x)] \, . \qquad (26)$$

Apply boundary conditions, and solve

$$c_1 = c_2 = \frac{\lambda_1 \lambda_2^2 \, \sigma_o (e^{\lambda c} + e^{-\lambda c} - 2)}{2k_o (\lambda_1^2 - \lambda_2^2) \{ (\lambda_1 - \lambda_2) \, [e^{-(\lambda_1 + \lambda_2)c} - e^{(\lambda_1 - \lambda_2)c}]}$$

$$\frac{1}{+ (\lambda_1 + \lambda_2) \, [e^{-(\lambda_1 - \lambda_2)c} - e^{(\lambda_1 - \lambda_2)c}] \}}$$

$$\cdot \, \{ [(\lambda_1 - \lambda_2) F(\lambda_1, c) + (\lambda_1 + \lambda_2) F(-\lambda_1, c) - 2\lambda_1 F(-\lambda_2, c)] e^{\lambda_2 c}$$

$$+ [(\lambda_1 + \lambda_2) F(\lambda_1, c) + (\lambda_1 - \lambda_2) F(-\lambda_1, c) - 2\lambda_1 F(\lambda_2, c)] e^{-\lambda_2 c} \} \, .$$

$$(27)$$

$$c_3 = c_4 = \frac{\lambda_1^2 \lambda_2 \, \sigma_0 (e^{\lambda c} + e^{-\lambda c} - 2)}{2k_0(\lambda_1^2 - \lambda_2^2)\{(\lambda_1 - \lambda_2)[e^{-(\lambda_1 + \lambda_2)c} - e^{(\lambda_1 + \lambda_2)c}]}$$

$$\frac{1}{+ (\lambda_1 + \lambda_2)[e^{-(\lambda_1 - \lambda_2)c} - e^{(\lambda_1 - \lambda_2)c}]\}} \cdot$$

$$\cdot \{[(\lambda_2 - \lambda_1)F(\lambda_2 c) + (\lambda_1 + \lambda_2)F(-\lambda_2, c) - 2\lambda_2 F(-\lambda_2, c)]e^{\lambda_1 c}$$

$$+ [(\lambda_1 + \lambda_2)F(\lambda_2, c) + (\lambda_2 - \lambda_1)F(-\lambda_2, c) - 2\lambda_2 F(\lambda_1, c)]e^{-\lambda_1 c}\}.$$

$$\tag{28}$$

$$w(x) = \frac{\lambda_1 \lambda_2 \, \sigma_0 (e^{\lambda c} + e^{-\lambda c} - 2)}{2k_0(\lambda_1^2 - \lambda_2^2)} \cdot$$

$$\cdot \left\{ \lambda_2 [F(\lambda_1, x) - F(-\lambda_1, x)] - \lambda_1 [F(\lambda_2, x) - F(-\lambda_2, x)] \right.$$

$$+ \lambda_2 (e^{\lambda_1 x} + e^{-\lambda_1 x}) \left(e^{\lambda_2 c}[(\lambda_1 - \lambda_2)F(\lambda_1, c) \right.$$

$$+ (\lambda_1 + \lambda_2)F(-\lambda_1, c) - 2\lambda_1 F(-\lambda_2, c)]$$

$$+ e^{-\lambda_2 c}[(\lambda_1 + \lambda_2)F(\lambda_1, c) + (\lambda_1 - \lambda_2)F(-\lambda_1, c)$$

$$\left. - 2\lambda_1 F(\lambda_2, c)] \right)$$

$$+ \lambda_1 (e^{\lambda_2 x} + e^{-\lambda_2 x}) \left(e^{\lambda_1 c}[(\lambda_2 - \lambda_1)F(\lambda_2, c) \right.$$

$$+ (\lambda_1 + \lambda_2)F(-\lambda_2, c) - 2\lambda_2 F(-\lambda_1, c)]$$

$$+ e^{-\lambda_1 c}[(\lambda_1 + \lambda_2)F(\lambda_2, c) + (\lambda_2 - \lambda_1)F(-\lambda_2, c)$$

$$\left. \left. - 2\lambda_2 F(\lambda_1, c)] \right) \right\}.$$

$$\tag{29}$$

2.2.4 <u>Results and Discussion</u> - Based upon the model and solution described above, a number of displacement fields and stress distributions for different parameters λ, λ_1, λ_2 have been obtained numerically and plotted as shown in Figures 5 and 6. In these plots, λ was taken to be 3 while λ_1 and λ_2 are 2 and 3, respectively. This simplified one-dimensional analysis shows quantitative similarity with results obtained from a two-dimensional analysis. This encourages further investigation of the stress distribution at and beyond the craze tip where the two-dimensional analysis indicates a similarity. By properly selecting the boundary conditions, solutions in closed form have been obtained. The singular condition will be considered by application of other mathematical techniques.

2.3 Prefracture Analysis of a Viscoelastic Craze in Solid Propellant Polymer

2.3.1 <u>Introduction</u> - Although crazing does not initially affect the polymer's load-carrying capacity, the propagation of crazes causes further deformation and eventually fracture. The mechanism of inception of crazing, propagation of crazes, nucleation of cracking and local stress distribution indicate that viscoelastic properties of the craze medium, as well as the bulk medium, play an important role in a complete analysis of the problem. An elastic model has been developed and reported in an earlier section of this report, and it is the object of this section to extend the result to the viscoelastic regime using linear viscoelastic models. It is obvious that the craze medium and the bulk medium undergo deformation at different rates, and they have different viscoelastic properties due to a difference in the degree of molecular orientation.

2.3.2 <u>Elastic Model</u> - Consider an infinite sheet of polymeric material under constant stress σ_o applied at infinity. This can be reduced to a one-dimensional problem when attention is confined to the craze boundary which is simulated by a bar bent to the same contour. The solution of the displacement field is

Figure 5. Craze Length vs. Craze Displacement
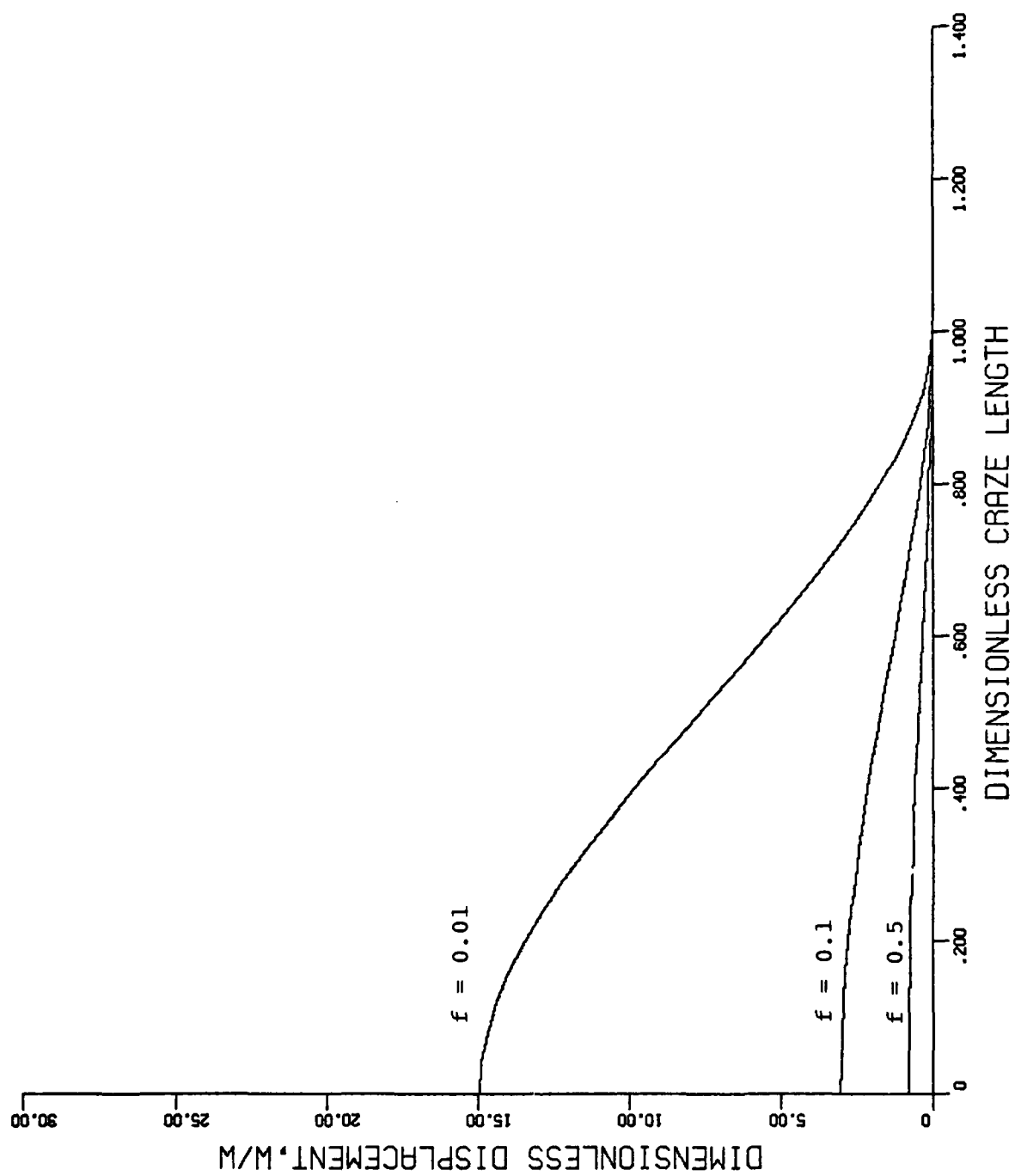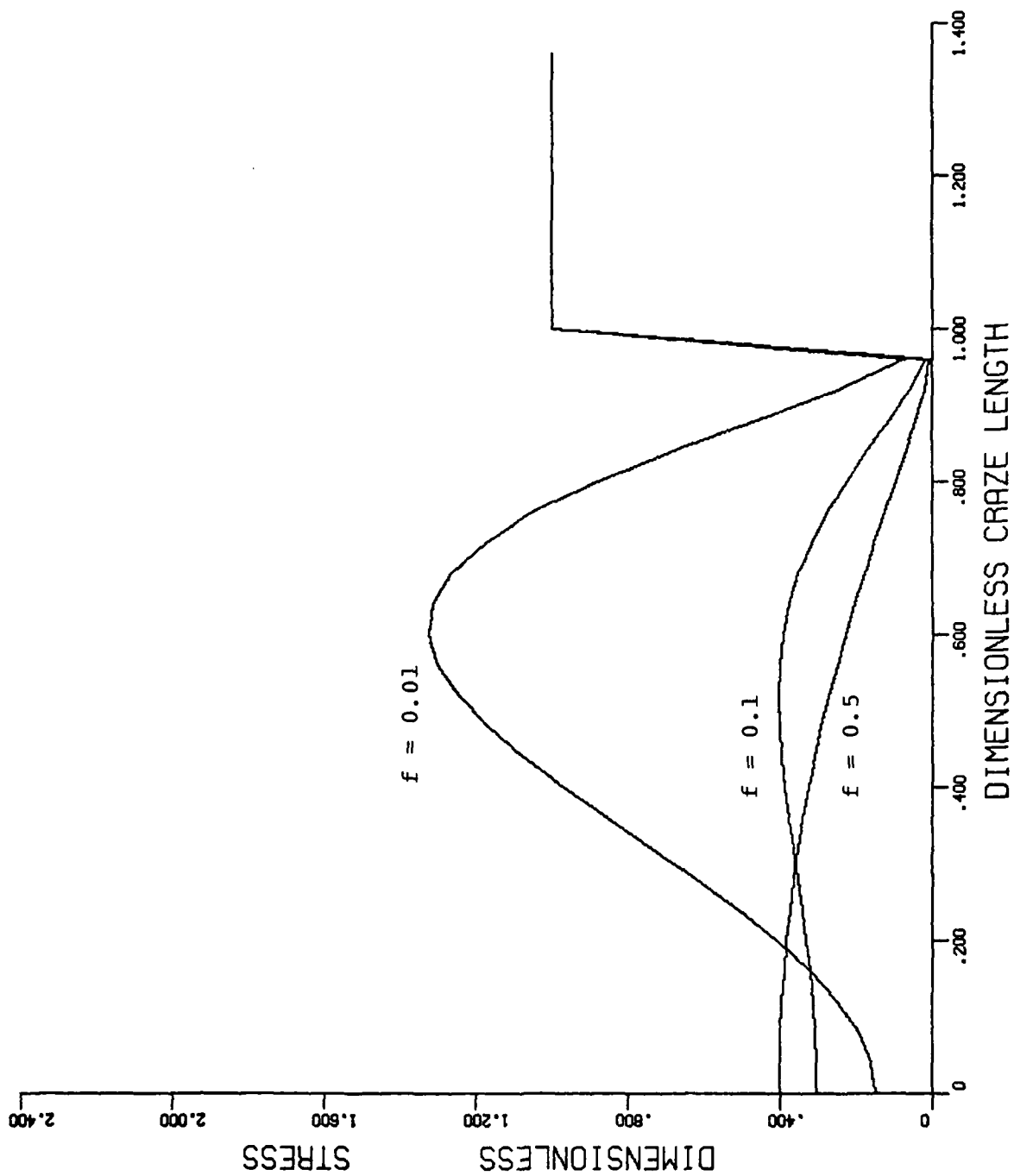
18

DIMENSIONLESS CRAZE LENGTH

f = 0.01

f = 0.1

f = 0.5

STRESS   DIMENSIONLESS

2.400
2.000
1.600
1.200
.800
.400
0

0   .200   .400   .600   .800   1.000   1.200   1.400

Figure 6. Craze Length vs. Stress Distribution

19

$$w(x) = \frac{\lambda_1 \lambda_2 \sigma_o (e^{\lambda c} + e^{-\lambda c} - 2)}{2k_o(\lambda_1^2 - \lambda_2^2)} \left\{ \lambda_2 \left[F(\lambda_1, x) - F(-\lambda_1, x) \right] - \lambda_1 \left[F(\lambda_2, x) - F(-\lambda_2, x) \right] \right.$$

$$+ \lambda_2 (e^{\lambda_1 x} + e^{-\lambda_1 x}) \left\{ e^{\lambda_2 c} \left[\lambda_1 - \lambda_2) F(\lambda_1, c) + (\lambda_1 + \lambda_2) F(-\lambda_1, c) - 2\lambda_1 F(-\lambda_2, c) \right] \right.$$

$$\left. + e^{-\lambda_2 c} \left[(\lambda_1 + \lambda_2) F(\lambda_1, c) + (\lambda_1 - \lambda_2) F(-\lambda_1, c) - 2\lambda_1 F(\lambda_2, c) \right] \right\}$$

$$+ \lambda_1 (e^{\lambda_2 x} + e^{-\lambda_2 x}) \left\{ e^{\lambda_1 c} \left[(\lambda_2 - \lambda_1) F(\lambda_2, c) + (\lambda_1 + \lambda_2) F(-\lambda_2, c) - 2\lambda_2 F(-\lambda_1, c) \right] \right.$$

$$\left. \left. + e^{-\lambda_1 c} \left[(\lambda_1 + \lambda_2) F(\lambda_2, c) + (\lambda_2 - \lambda_1) F(-\lambda_2, c) - 2\lambda_2 F(\lambda_1, c) \right] \right\} \right\}$$

(30)

where λ_1, λ_2, λ, c are constants as reported earlier.

2.3.3 Viscoelastic Model - In the above solution of displacement field of the craze boundary, the quantities which are time dependent are applied stress, $\sigma_o(t)$, modulus function of bulk medium, $k_o(t)$, and the function $f(t)$ which appears under function $F(y,x,t)$.

So the time dependent displacement field is

$$w(x,t) = \frac{\lambda_1 \lambda_2 \sigma_o(t) [e^{\lambda c} + e^{-\lambda c} - 2]}{2k_o(t)(\lambda_1^2 - \lambda_2^2)} \left\{ \lambda_2 [F(\lambda_1, x, t) - F(-\lambda_1, x, t)] - \lambda_1 [F(\lambda_2, x, t) - F(-\lambda_2, x, t)] \right.$$

$$+ \lambda_2 (e^{\lambda_1 x} + e^{-\lambda_1 x}) \left\{ e^{\lambda_2 c} [(\lambda_1 - \lambda_2) F(\lambda_1, c, t) + (\lambda_1 + \lambda_2) F(-\lambda_1, c, t) - 2\lambda_1 F(-\lambda_2, c, t)] \right.$$

$$\left. + e^{-\lambda_2 c} [(\lambda_1 - \lambda_2) F(\lambda_1, c, t) + (\lambda_1 - \lambda_2) F(-\lambda_2, c, t) - 2\lambda_1 F(\lambda_2, c, t)] \right\}$$

$$+ \lambda_1 (e^{\lambda_2 x} + e^{-\lambda_2 x}) \left\{ e^{\lambda_1 c} [(\lambda_2 - \lambda_1) F(\lambda_2, c, t) + (\lambda_1 + \lambda_2) F(-\lambda_2, c, t) - 2\lambda_2 F(-\lambda_1, c, t)] \right.$$

$$\left. \left. + e^{-\lambda_1 c} [(\lambda_1 + \lambda_2) F(\lambda_2, c, t) + (\lambda_2 - \lambda_1) F(-\lambda_2, c, t) - 2\lambda_2 F(\lambda_1, c, t)] \right\} \right\}$$

(31)

By Laplace transformation, the displacement field in the Laplace domain is

$$\overline{w}(x,s) = \frac{\lambda_1\lambda_2\overline{\sigma}_o(s)(e^{\lambda c}+e^{-\lambda c}-2)}{2k_o(s)(\lambda_1^2-\lambda_2^2)}\left\{\lambda_2[\overline{F}(\lambda_1,x,s)-\overline{F}(-\lambda_1,x,s)]-\lambda_1[\overline{F}(\lambda_2,x,s)-\overline{F}(-\lambda_2,x,s)]\right.$$

$$+\lambda_2(e^{\lambda_1 x}+e^{-\lambda_1 x})\left\{e^{\lambda_2 c}[(\lambda_1-\lambda_2)\overline{F}(\lambda_1,c,s)+(\lambda_1+\lambda_2)\overline{F}(-\lambda_1,c,s)-2\lambda_1\overline{F}(-\lambda_2,c,s)]\right.$$

$$\left.+e^{-\lambda_2 c}[(\lambda_1+\lambda_2)F(\lambda_1,c,s)+(\lambda_1-\lambda_2)\overline{F}(-\lambda_2,c,s)-2\lambda_1\overline{F}(\lambda_2,c,s)]\right\}$$

$$+\lambda_1(e^{\lambda_2 x}+e^{-\lambda_2 x})\left\{e^{\lambda_1 c}[(\lambda_2-\lambda_1)\overline{F}(\lambda_2,c,s)+(\lambda_1+\lambda_2)\overline{F}(-\lambda_2,c,s)-2\lambda_2\overline{F}(-\lambda_1,c,s)]\right.$$

$$\left.\left.+e^{-\lambda_1 c}[(\lambda_1+\lambda_2)\overline{F}(\lambda_2,c,s)+(\lambda_2-\lambda_1)\overline{F}(-\lambda_2,c,s)-2\lambda_2\overline{F}(\lambda_1,c,s)]\right\}\right\} \quad (32)$$

$$\text{where}\quad \overline{F}(y,x,s) \equiv \int_0^x \frac{e^{y(x-\xi)}}{\overline{f}(s)(e^{\lambda c}+e^{-\lambda c})-2+[1-\overline{f}(s)](e^{\lambda\xi}+e^{-\lambda\xi})}d\xi, \quad (33)$$

where $k_o(t)$ is the modulus of the bulk medium, i.e., before a craze is developed in it. Dividing the modulus of elasticity $E(x,t)$ of the bulk medium by a characteristic length, say h, gives the spring constant or elastic foundation constant k_o. Before a craze initiates, the displacement w_o of an imaginary plane under uniform stress σ_o is given by

$$w_o = \frac{\sigma_o}{k_o} \quad (34)$$

$$\text{where}\quad k_o(t) = \frac{E(x,t)}{h} \quad (35)$$

where h is a constant.

So $k_o(t)$ has identical time-dependent properties as $E(x,t)$. Now

$$k(x,t) = k_o(t)\left(f(t) + [1-f(t)]\frac{e^{\lambda x}+e^{-\lambda x}-2}{e^{\lambda c}+e^{-\lambda c}-2}\right) \quad (36)$$

where $k(x,t)$ is the time dependent modulus function of craze medium.

Physically $k(x,t)$ depends on displacement $w(x,t)$ and the nonlinear visco-elastic nature of $k(x,t)$ can be predicted. From the above definition of $k(x,t)$ it is obvious that nonlinear properties come from the function $f(t)$ which also depends on $w(x,t)$.

Therefore, it may be concluded that the bulk medium outside craze region is linearly viscoelastic while the craze medium is nonlinearly viscoelastic.

The stress applied at infinity, $\sigma_o(t)$, is constant so it can be represented by a unit step function,

$$\sigma_o(t) = \sigma_o \ u(t) \tag{37}$$

By Laplace transformation

$$\bar{\sigma}_o(s) = \frac{\sigma_o}{s} \tag{38}$$

$E(x,t)$ and $k_o(t)$ are linearly viscoelastic quantities.

By linear viscoelasticity in the Laplace domain

$$P_V \bar{\sigma}_{ii}(s) = Q_V \bar{\varepsilon}_{ii}(s) \ \text{———} \ \text{Volume Behavior}, \tag{39}$$

$$P_S \bar{s}_{ij}(s) = Q_S \bar{e}_{ij}(s) \ \text{———} \ \text{Shear Behavior} \tag{40}$$

where $\bar{\sigma}_{ii}$, $\bar{\varepsilon}_{ii}$ are normal stress and strains,

$\bar{s}_{ij}$, $\dot{e}_{ij}$ are deviatoric stresses and strains,

P_V, Q_V, P_S, Q_S are viscoelastic operators in the Laplace domain.

In elasticity

$$\sigma_{ii} = 3\bar{K} \ \varepsilon_{ii} \tag{41}$$

$$s_{ij} = 2\bar{G} \ e_{ij} \tag{42}$$

where K is bulk modulus and G is shear modulus.

By analogy

$$\frac{Q_V}{P_V} \sim 3K \tag{43}$$

$$\frac{Q_S}{P_S} \sim 2G \ . \tag{44}$$

22

By theory of elasticity

$$E = \frac{9KG}{3K + G} .$$ (45)

So, by the principle of correspondence in the viscoelastic regime,

$$\overline{E}(x,s) = \frac{9(\frac{1}{3} Q_v/P_v)(\frac{1}{2} Q_s/P_s)}{Q_v/P_v + \frac{1}{2} Q_s/P_s} = \frac{\frac{3}{2}(Q_v/P_v)(Q_s/P_s)}{Q_v/P_v + \frac{1}{2} Q_s/P_s} .$$ (46)

Taking the Laplace transformation of Equation 35

$$\overline{k}_o(s) = \frac{\overline{E}(x,s)}{h}.$$ (47)

Assume that the volume behavior of the bulk medium is elastic and that the shear behavior is represented by a Maxwell model.

$$\sigma_{ii}(t) = 3K_B \varepsilon_{ii}(t) ,$$ (48)

$$s_{ij}(t) + \frac{\eta_B}{k_B} \frac{\partial}{\partial t} s_{ij}(t) = \eta_B \frac{\partial}{\partial t} e_{ij}(t) ,$$ (49)

where subscript B denotes properties of bulk medium.

k and η are the spring constant and damping coefficient of the mathematical model respectively.

By Laplace transformation

$$\overline{\sigma}_{ii}(s) = 3\overline{K}_B \overline{\varepsilon}_{ii}(s) ,$$ (50)

$$\overline{s}_{ij}(s) + \frac{\overline{\eta}_B}{\overline{k}_B} s \overline{s}_{ij}(s) = \overline{\eta}_B s \overline{e}_{ij} ,$$ (51)

so $\quad \frac{Q_v}{P_v} = \frac{\overline{\sigma}_{ii}(s)}{\overline{\varepsilon}_{ii}(s)} = 3\overline{K}_B ,$ (52)

$$\frac{Q_s}{\overline{P}_s} = \frac{\overline{s}_{ij}(s)}{\overline{e}_{ij}(s)} = \frac{\overline{\eta}_B \, s}{\overline{k}_B + \overline{\eta}_B \, s} \tag{53}$$

$$\overline{E}(s) = \frac{\frac{3}{2}(3\overline{K}_o)(\overline{\eta}_B s/\overline{k}_B + \overline{\eta}_B s)}{3\overline{K}_B + \frac{1}{2}\overline{\eta}_B s/\overline{k}_B + \overline{\eta}_B s} = \frac{9\overline{K}_B \, \overline{\eta}_B s}{6\overline{K}_B\overline{k}_B + (6\overline{K}_B+1)\overline{\eta}_B}, \tag{54}$$

and $\sigma(x,t) = k(x,t) \, w(x,t) = k(x,t) \, h \, \varepsilon(x,t)$ (55)

$$k(x,t) = \frac{1}{h}\frac{\sigma(x,t)}{\varepsilon(x,t)} \tag{56}$$

For nonlinear viscoelasticity the stress-strain relationship can be obtained by use of the absolute reaction rate theorem.

For the Maxwell model,

$$\dot{\varepsilon}(t) = \frac{1}{k_c}\dot{\sigma}(t) + \zeta(t) \sinh \frac{\gamma\sigma(t)}{kT} \tag{57}$$

where subscript c denotes craze medium and kT represents thermoenergy, γ is a material constant and $\zeta(t)$ is a time dependent function.

2.3.4 <u>Result and Solution</u> - By choosing an appropriate model for the non-linear viscoelastic behavior of the craze medium, $\overline{k}(x,t)$ can be solved from Equation 56. Then with an appropriate choice of linear viscoelastic model for the bulk medium $\overline{E}(x,s)$ and $\overline{k}_o(s)$ are obtained, and $k_o(t)$ is determined by Laplace inversion. The result is then substituted into Equation 36, which is solved for $f(t)$. After $f(t)$ is obtained, $\overline{f}(s)$ is determined and $\overline{F}(y,x,s)$ is solved for from Equation 34. With known $\overline{\sigma}_o(s)$, $\overline{k}_o(s)$, $\overline{F}(y,x,a)$ and $\overline{E}(s)$, $\overline{w}(x,s)$ can be solved from Equation 33 and $w(x,t)$ is solved by Laplace inverse transformation.

2.4 Measurement of In-Plane Displacements of Propellant Polymer Craze by Speckle Technique

It has been known for some time that, in speckle interferometry, in principle one can magnify the original speckle size and record a magnified speckle pattern on a photographic negative. This section will describe how it has been done in the laboratory and will present some results. It will also point out a few technical details one should pay attention to when using this technique.

24

The authors have been using speckle interferometry to find the displacement field along the boundary of a craze or a crack. A craze is created in a propellant polymer specimen. The speckle pattern is formed by illuminating the craze boundary in the specimen under two different states of applied stress with a laser beam and using a double exposure technique to record the interference pattern so formed on a photographic negative. It is desired to measure the displacement fields at as many points as possible, especially near the craze tip region. Hence it is desirable to obtain an enlarged speckle pattern for a small region, so that the fringes can be constructed at many different positions in this small region. Using the well-known relationship:

$$d = \frac{\lambda L}{Mh} \tag{58}$$

where d = displacement between two applied loads,

λ = wavelength of laser,

L = distance between the speckle pattern and the fringe image plane,

M = magnification factor or speckle pattern,

and h = pitch of the fringes,

the displacement field due to applied stress can be obtained.

The photographic system used is illustrated by Figure 7; a schematic diagram of the system is shown in Figure 8. A microscope is placed along the reflected beam of the specimen, the image of which goes directly to the camera. NOTE: every component of the system must be fixed in position and any relative movement between laser source, specimen, microscope and camera will distort the speckle pattern. All the lenses, specimen, and recording negative are aligned perpendicular to the laser beam. One essential thing to be noted when a speckle pattern is recorded is that the photographic negative has to be placed at the exact position where the interference pattern is formed. Since there is a slight shift in positions between the plane on which one views the image in a camera and the actual position of the negative, the image must be adjusted to an apparent out of focus position when viewed through the camera. This compensates the shift and will place the negative at the exact position of the interference pattern. As to the question of how far off-focus should it be, this has to be answered by experience since it may differ from one photographic system to another. Exact compensation is especially critical here since a
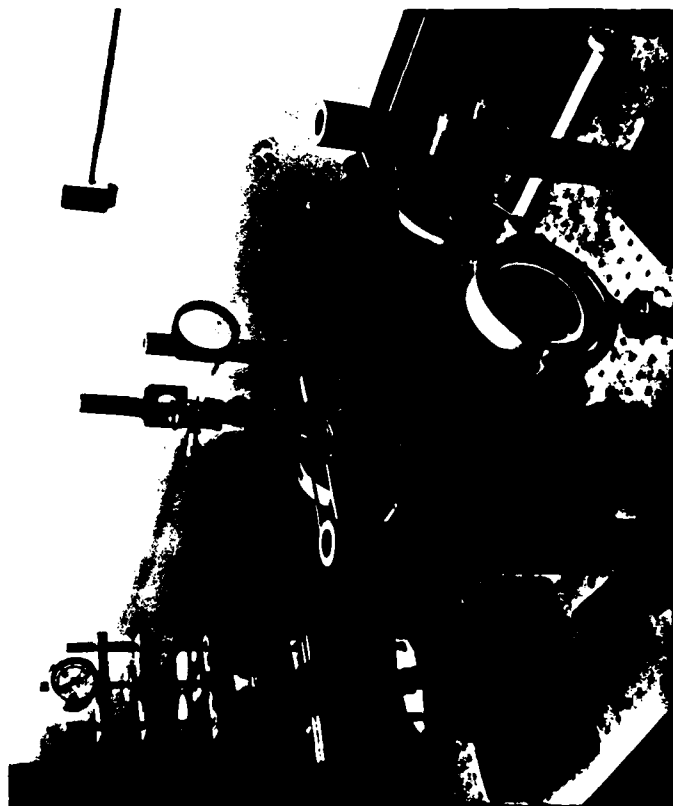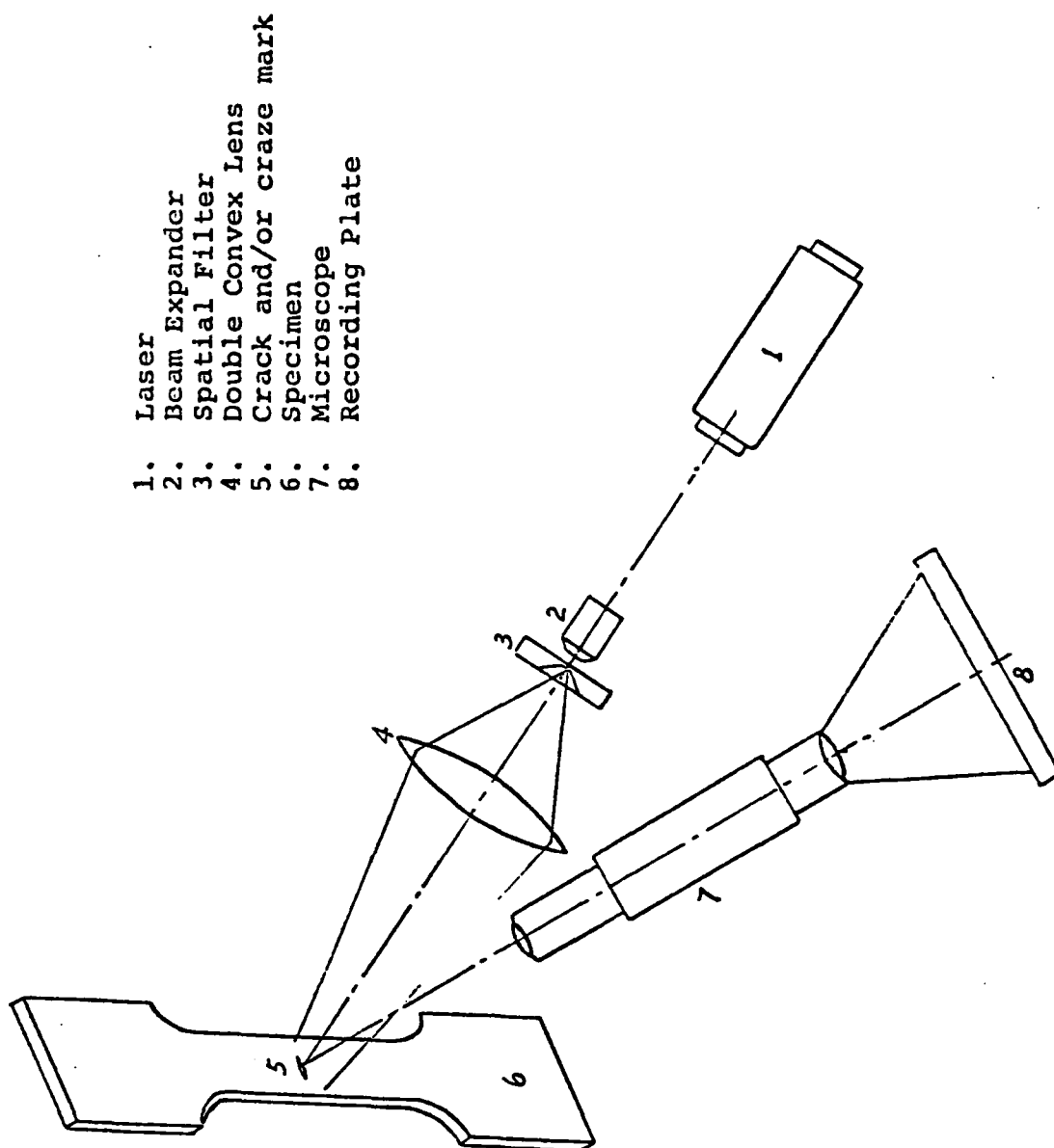
25

Figure 7. Laser Speckle Interferometric System

1. Laser
2. Beam Expander
3. Spatial Filter
4. Double Convex Lens
5. Crack and/or craze mark
6. Specimen
7. Microscope
8. Recording Plate

Figure 8. Schematic Diagram of Microspeckle System

27

microscope is used to magnify the incident beam before it falls on the
recording negative. The microscope produces a magnified interference pattern
exactly at the focal length of the eye-piece. Any error in positioning the
negative may cause a large distortion of the speckle pattern.

Figures 9a through 11a are the speckle patterns recorded with the incident
beam magnified by one, three and 10 times for propellant polymer specimen,
respectively.   Figures 9b through 11b are the corresponding fringes
obtained near the craze tip in the specimen. It is noted that higher magnifi-
cation factor lowers the contrast and distinction of the Young's fringes.
Another disadvantage of this microspeckle method is that the magnitude of
applied stress and strain (between two exposures) is limited since each
speckle pattern covers only a very small region on the specimen. This is
especially important for rubber specimens where large deformation is usually
encountered. However, the magnification factor can be increased, if desired,
by using a microscope of higher resolving power and magnification factor. The
double convex lens placed behind the spatial filter is not necessary if the
laser source is strong enough (the one used here is 0.05 mW He-Ne laser).

The present system has room for improvements.

2.5 Prefracture Behavior of Polymer Systems

2.5.1 Introduction - During the past thirty odd years a great deal of
knowledge has been accumulated on the development of crazing in brittle polymers
in a tensile stress field. Five excellent reviews of craze and fracture in
polymers summarizing a wide variety of experimental observations and physical
models have appeared (1,2,3,4,5). It is generally accepted that glassy polymer
fracture proceeds in the following sequences:

1. R. P. Kambour: J. Polymer Sci. D (Reviews) 7, 1 1973.
2. S. Rabinowitz, P. Beardmore: CRC Critical Reviews 1, 1 1973.
3. W. G. Knauss, Applied Mechanics Reviews 1 1973, 1-17.
4. H. H. Kausch, Polymer Fracture, Spring-Verlag Berlin Heidelberg New York,
   1978.
5. Edward J. Kramer, "Developments in Polymer Fracture -1" ed by E. H. Andrews,
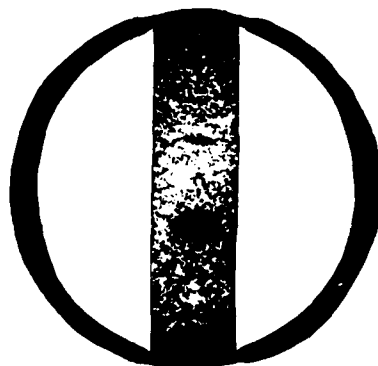   Applied Science Publishers LTD, London, 55, 1979.

Figure 9a. Specklegram of Propellant Polymer 1X
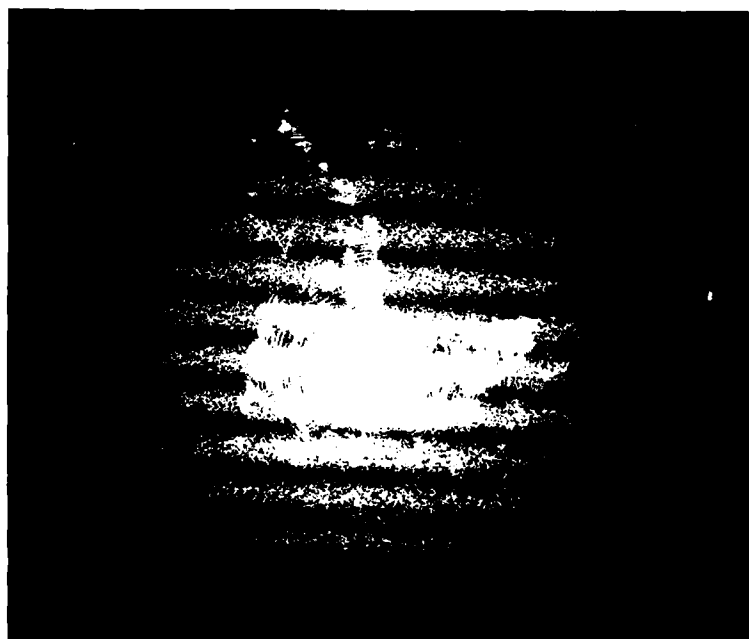

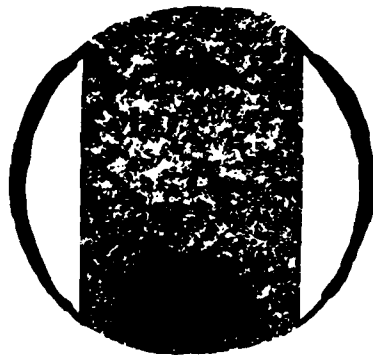Figure 9b. Fringe pattern near Craze Tip

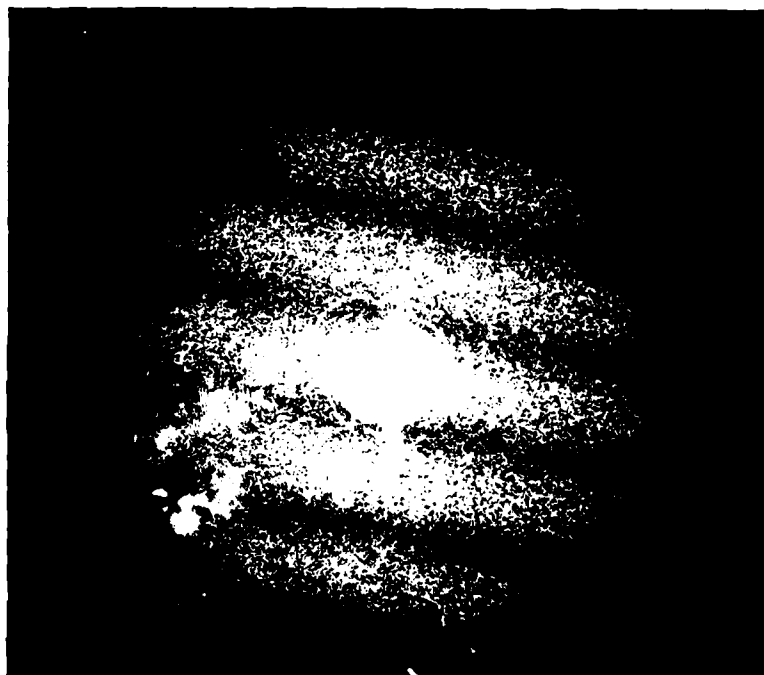Figure 10a. Specklegram of Propellant Polymer 3X
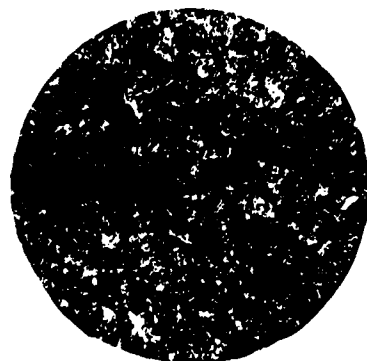

Figure 10b. Fringe Pattern near Craze Tip
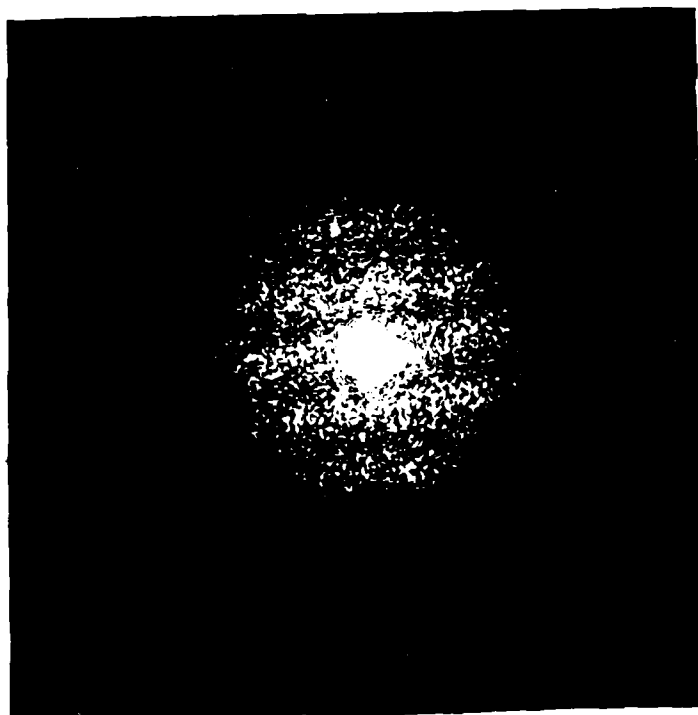
Figure 11a. Specklegram of Propellant Polymer 10X

Figure 11b. Fringe Pattern near Craze Tip

(i)   At sites of stress concentrations or defects such as cracks, flaws, inhomogenities, particle inclusions and environmental softening zones, crazes nucleate well before fractures;

(ii)   With sustained local large straining, a craze continues to grow and deform internally;

(iii)   Eventually cracks develop usually at the central region of individual crazes;

(iv)   Subsequently, these cracks propagate behind the craze tips by repeating somewhat similar processes as described above.

Up to now most of the continuum mechanics models used for analyzing prefracture craze behavior are based upon a generalized Dugale crack with a plastic zone at each tip (5,6,7). The plastic zone is considered as a region of craze. Methods in linear fracture mechanics for elastic media have been employed for analyses. Schapery in a series of papers (8,9,10,11,12) employed the concept of conservation of work and fracture energy criterion and generalized Dugdale model for linear viscoelastic materials. All these considerations are based upon the assumption that the length of the craze zone (same as the failure zone or plastic zone) is negligible compared with that of the crack. Thus the craze growth velocity, crack growth initiation time and its propagation velocity are governed by a crack induced stress intensity factor.

In prefracture processes of polymeric systems crazing occurs usually before any cracking. Thus the assumption that the crack length is much larger than the craze region is no longer adequate. Therefore the application of the fracture mechanics method directly in analyzing this complex occurence is unlikely to be satisfactory. As a result a new approach is considered. In this report, the above assumption is eliminated from

6. Happel, J. and Brenner, H. Low Reynolds Number Hydrodynamics, Prentice-Hall International, Hemel-Hempstead, Herts, 395, 1965.
7. Gerberich, W. W. International J. of Fracture, 13, 55 1977.
8. R. A. Schapery. Int. Journal of Fracture, 11, 144, 1975.
9. R. A. Schapery. Int. Journal of Fracture, 11, 369, 1975.
10. R. A. Schapery. Int. Journal of Fracture, 11, 549, 1975.
11. R. A. Schapery. Int. Journal of Fracture, 14, 293, 1975.
12. R. A. Schapery. SIAM - Ams Proceedings 12, 137, 1979.

consideration. In addition the entire local deformation behavior responsible for craze-thickening and load-bearing characteristics is taken into account in formulating a new mathematical model. This is necessary if a better understanding of the craze mechanism, the transformation of the polymer matrix into a new phase (craze material with voids) is to be obtained. Fundamental properties such as the molecular orientation strength of the polymer and the breakage rate of the molecular bundles should be considered in a complete endeavor.

Knight (13) and Kramer (5) utilized a Fourier transform method for crack analysis and introduced either an assumed or measured displacement field of a craze profile to calculate the stress distribution. Verhuelpen-Heymans and Bauwens (14) assumed a two-step stress distribution and used Muskhelishvili's complex variable technique (15) to calculate the displacements of a craze. In these cases the problem has been treated mathematically as either a first boundary value problem with prescribed traction forces or the second boundary value problem with prescribed displacements. In both cases the initial shape of a crack has been considered as its boundary with singular crack tips. However, in the present analysis, the load-bearing molecular bundles reduce the singular nature of stress concentration at craze tips. The new model developed predicts both the displacements and the stress distribution along the prefracture craze envelope.

2.5.2 Model Analysis - The occurence of crazes in many stressed polymers is a common phenomenon. According to the current understanding the formation of an individual craze comes about as a physical transformation in the deformation processes from an original phase to a new phase with oriented molecules and voids. Each craze is usually quite similar to any other. This suggests the possibility of analyzing the vicinity of a single craze by considering a symmetrical double beam as shown in Figure 12. AABB shows a quarter section of the augmented double beam containing a thin primordial

13. A. C. Knight. J. Polymer Sci. 3 1845, 1965
14. Verhuelpen-Heymens, N. and J. C. Bauwens, J. Materials Sci. 11 7, 1976
15. N. I. Muskhelishvili, "Some Basic Problems of Mathematical Theory of Elasticity", Neordhoff, Groningen, The Netherlands, 340, 1953.
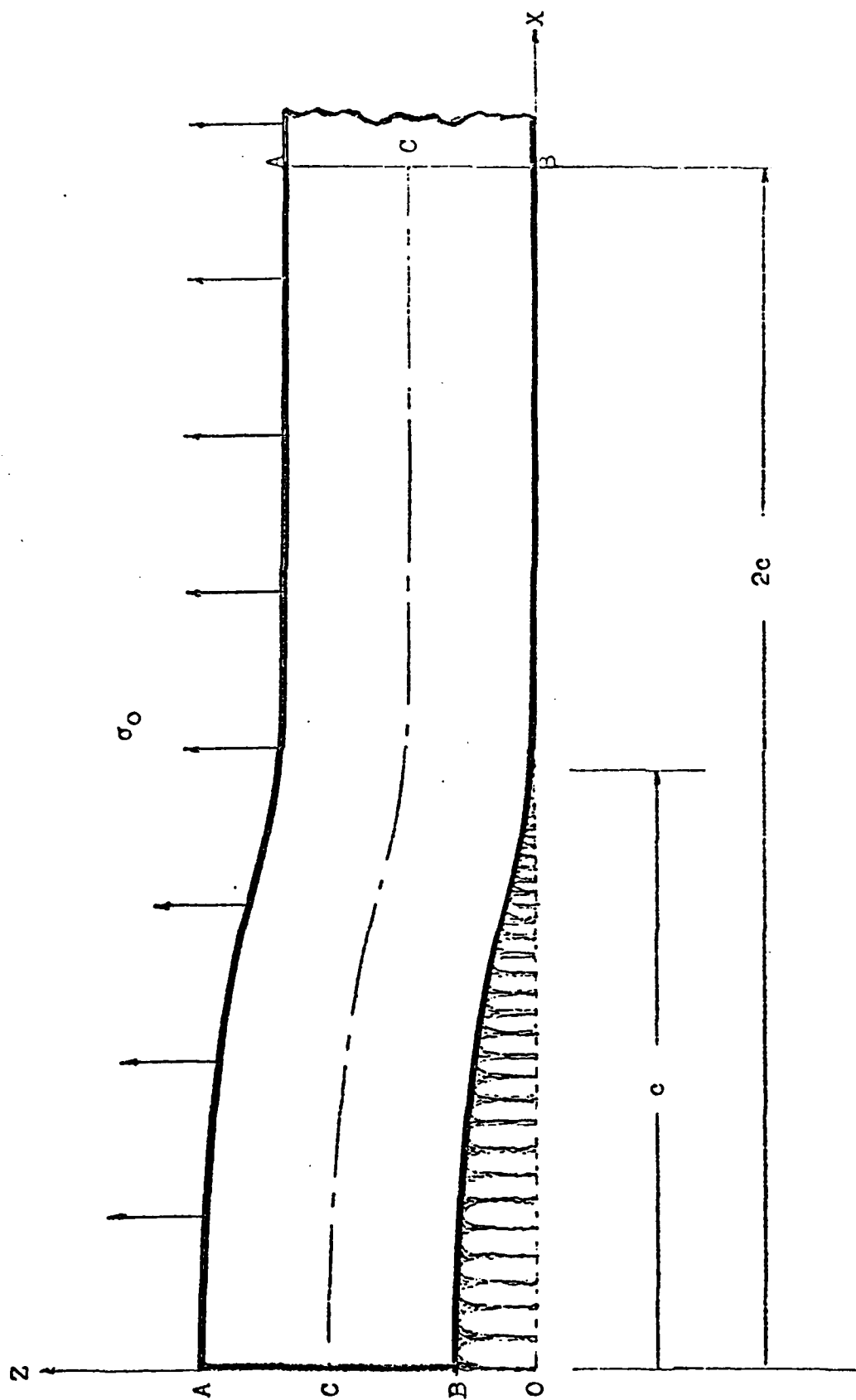
Figure 12. Double Augmented Beam Model Showing the Vicinity of a Quadrantal Craze

34

craze layer next to BB which has transformed into the new phase resisting both the normal and shear deformation. The mathematical equation governing the vertical displacement $w(x)$ of the center line CC for the uniform beam AABB of unit thickness is:

$$EI\nabla^2\nabla^2 w - S(x)\nabla^2 w + K(x)w = \sigma_o \qquad (59)$$

where E is the modulus of elasticity of the beam,

I is the second moment of the cross-section of the beam,

$\nabla^2 \equiv \partial^2/\partial x^2$ is the del operator,

S is the shear foundation modulus,

K is the elongation foundation modulus,

and σ_o is the applied stress.

With the following boundary conditions:

$$w'(0) = w'''(0) = w''(2c) = w'''(2c) = 0 \qquad (60)$$

where the primed quantities represent their derivitives with respect to the length of the craze. Equation 59 can be solved by finite difference methods for any foundation modulus function. That is, Equation 59 can be rewritten as normal first-order system

$$w'''' = [S(x)w'' - K(x)w + \sigma_o]/EI, \qquad (61)$$

or, in matrix form,

$$d[W]/dx = [A][W] + [B] \qquad (62)$$

where

$$[W] = \begin{pmatrix} w \\ w' \\ w'' \\ w''' \end{pmatrix} ,$$

(63)

$$[A] = \begin{pmatrix} 0 & 0 & 0 & 0 \\ 0 & 1 & 0 & 0 \\ 0 & 0 & 1 & 1 \\ \dfrac{-K(x)}{EI} & 0 & \dfrac{S(x)}{EI} & 0 \end{pmatrix} ,$$

(64)

$$[B] = \begin{pmatrix} 0 \\ 0 \\ 0 \\ \dfrac{\sigma_o}{EI} \end{pmatrix} .$$

(65)

The boundary condition is

$$[C][W]_{x=0} + [D][W]_{x=2c} = [E]$$

(66)

where

$$[C] = \begin{pmatrix} 0 & 1 & 0 & 0 \\ 0 & 0 & 0 & 1 \\ 0 & 0 & 0 & 0 \\ 0 & 0 & 0 & 0 \end{pmatrix} ,$$

(67)

$$[D] = \begin{pmatrix} 0 & 0 & 0 & 0 \\ 0 & 0 & 0 & 0 \\ 0 & 0 & 1 & 0 \\ 0 & 0 & 0 & 1 \end{pmatrix} ,$$

(68)

$$[E] = \begin{pmatrix} 0 \\ 0 \\ 0 \\ 0 \end{pmatrix}. \tag{69}$$

Equations 62 and 66 together with the given foundation modulus functions $K(x)$ and $S(x)$ can be solved by the implementation of computer programming for obtaining the displacement field $w(x)$.

This approach, based upon a simple model, has been checked numerically for some polymer systems. Results have shown encouraging agreements while the prefracture problem is extremely complicated. Applications of this theory to propellant polymers are reported later.

2.5.3 Further Details - Considering that the thickness of the premordial craze as 2e then the elongation foundation modulus varies as a function of the development of the new phase. For craze and uncraze regions respectively:

$$K(x) = \frac{2E}{h + e(x)\left(\dfrac{E}{E_c} - 1\right)} \qquad (0 \leq x \leq c) \tag{70}$$

where E_c is the modulus of elasticity in the craze region.

$$K(x) = \frac{2E}{h}, \qquad (c \leq x \leq 2c) \tag{71}$$

If K is the constant elongation modulus, then

$$K(x) = q(x) K, \qquad (0 \leq x \leq c) \tag{72}$$

$$K(x) = K, \qquad (c \leq x \leq 2c) \tag{73}$$

where $q(x) = \left[1 + \dfrac{e(x)}{h}\left(\dfrac{E}{E_c} - 1\right)\right]^{-1}.$ \tag{74}

The shear foundation modulus varies as follows:

$$S(x) = 0, \qquad (0 \leq x \leq c) \tag{75}$$

37

$$S(x) = \delta hG \qquad\qquad (c \leq x \leq 2c) \qquad (76)$$

where δ is a proportional constant and G is the shear modulus of the uncrazed medium.

2.6 Effect of Ammonium Perchlorate on Prefracture Behavior of Propellant Polymer

2.6.1 <u>Introduction</u> - The objectives of this work are to develop a mathematical model which predicts prefracture behavior of solid propellants under load and to establish whether a definable relationship exists between craze or microflaw development and subsequent crack propagation in solid propellants. This effort will contribute to the reliability of missile propulsion systems by developing a theoretical understanding of the processes leading to propellant cracking.

Currently a two-dimensional mathematical model has been developed for analyzing individual crazes using infinitesimal elasticity theory. However, in order to fit to systems with large deformations a "one-dimensional" mathematical model has been developed for describing two-dimensional plane crazes. Based upon the use of "clamped" double cantilever beams the displacement field between the beams has been calculated as a result of applied stress as well as functions of the modulus of elasticity of the medium, the thickness of each beam, the magnitude of shear and the variation of the strength of the oriented polymer as the prescribed boundary conditions of a craze.

It was found that under a constant tensile stress the displacements of a craze increase in magnitude as the percentage of ammonium perchlorate in the propellant polymer increases. The geometrical shapes of the craze were observed to agree fairly well with the analytical predictions.

2.6.2 <u>Analysis</u> - One-dimensional double augmented beams are used to simulate the two-dimensional plane craze as shown in Figure 13. A uniform tensile stress σ_o is applied. At the craze region a new phase of oriented molecules with voids is developed. They act as prescribed boundary resistance forces on the surface of craze. For properly describing the craze opening,
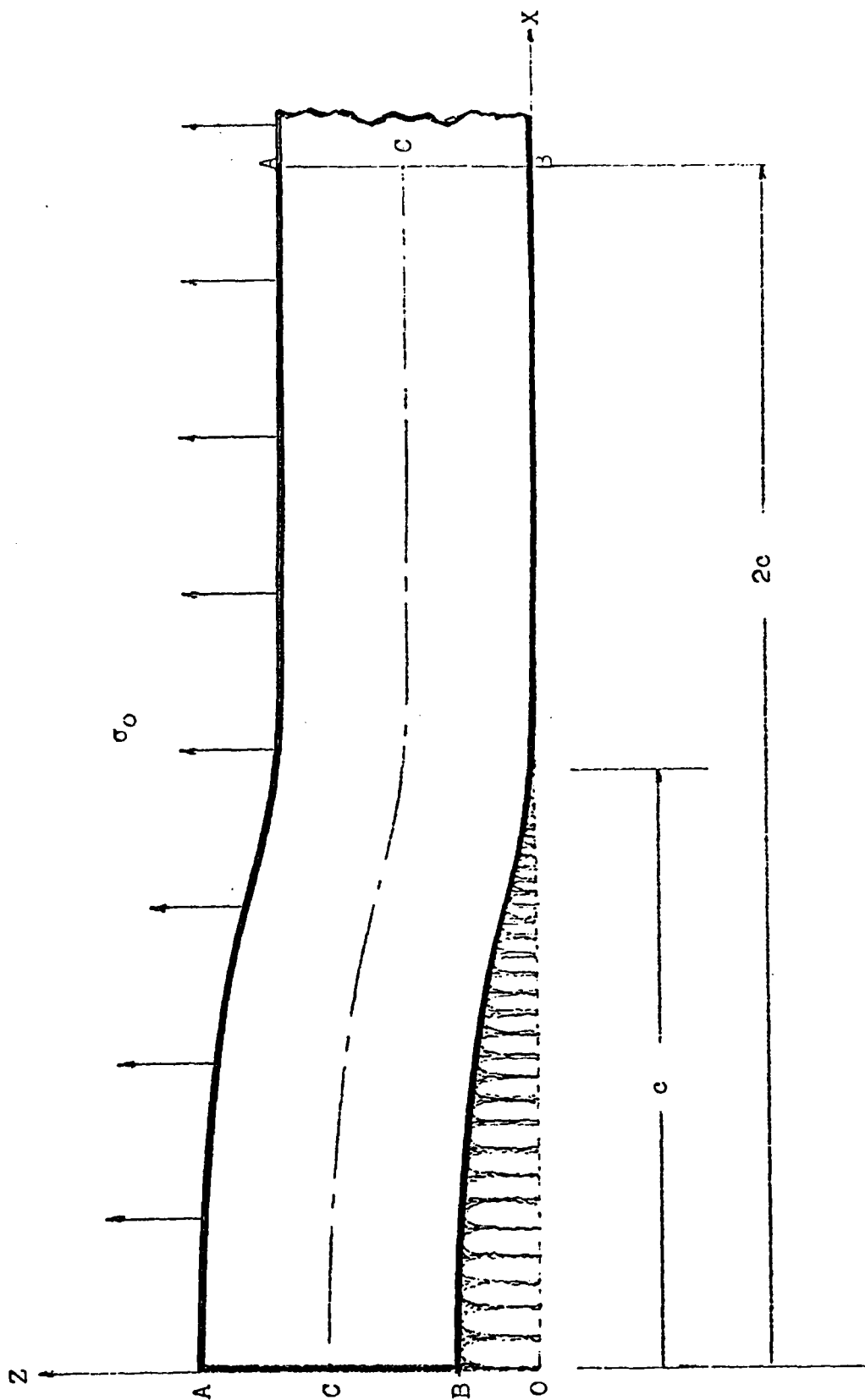
Figure 13. Double Augmented Beam Model Showing the Vicinity of a Quadrantal Craze

39

the basic equation determining the deflection of a beam on an elastic foundation is utilized:

$$EI\nabla^2\nabla^2 w - G\delta h\nabla^2 w + K(x)w = \sigma_o \tag{77}$$

where E is the modulus of elasticity of the polymer,

  I is $h^3/12$, the second moment of the beam cross-section per unit width,

  w is the vertical displacement,

  G is shear modulus,

  δ is a fraction,

  h is the height of each split beam,

and K(x) is the modulus of elasticity of the craze material in the new phase.

  By considering a continuous variation of the modulus function k(x), the application of the calculus of variation reveals that for a beam of 2c in length where c represents the craze length the modulus function varies as follows:

$$k(x) = k_o[f + (1 - f)(e^{\lambda x} + e^{-\lambda x} - 2)/(e^{\lambda c} + e^{-\lambda c} - 2)],$$

$$(0 \le x \le c)$$

$$k(x) = k_o \qquad (c \le x \le 2c) \tag{78}$$

where f is a fraction identifying the density of the craze medium,

  λ is a constant,

and k_o is the modulus function of the polymer without craze. It is easily verified that

$$k_o = \frac{2E}{h}. \tag{79}$$

  With the following boundary conditions

$$w'(0) = w'''(0) = w''(2c) = w'''(2c) = 0, \tag{80}$$

Equation 77 can be solved by finite-difference method.

2.6.3 <u>Experimental Results</u> - Assuming that $h/c \cong 0.2$, $\delta \cong 0.1$, and $\lambda \cong 3$, a number of displacement and stress distributions have been obtained for propellant polymers containing different amounts of ammonium perchlorate particles.

Specimens having three percentages of ammonium perchlorate have been tested in a universal testing unit and true stresses and true strains have been calculated.

Referring to Figure 14 for all the specimens tested, it was found that the modulus of elasticity for the initial portion of the stress-strain curve was essentially constant. The propellant polymer was composed of cured HTPB binder containing small percentages of ultra-fine ammonium perchlorate (AP).

For specimens with 0% AP, $E \cong 142$ psi.

For specimens with 2% AP, $E = 94.2$ psi.

For specimens with 10% AP, $E \cong 75$ psi.

The sample specimens were die cut from thin cast sheets with nominal thickness of about 3/32".

The true stress was determined on the basis that the volume of the sample specimen was assumed constant throughout the duration of testing. Thus the load divided by the instantaneous cross-sectional area gives the true stress value. As for the true strain values, the logarithm of the length ratios has been calculated. The original gage length chosen was 2". Figure 15 shows the dimensions of a die cut propellant polymer specimen.

In order to see the effect of the percentage of ammonium perchlorate particles (6μ) on the displacements of a craze, Figure 16 shows their influence under a constant stress of 20 psi.

Figures 17-19 respectively show the displacement field for 0, 2 and 10% ammonium perchlorate under different stresses as indicated.

For the purpose of observing the influence of the density variation of the craze medium Figures 20 - 22 respectively show the f quantities as affected by 0, 2 and 10% ammonium perchlorate under a same stress of 30 psi.

2.6.4 <u>Remarks</u> - Referring to Figure 24 it is seen that there are numerous small crazes developed on the surface of the propellant polymer containing 2% ammonium perchlorate. The big craze had been helped to grow
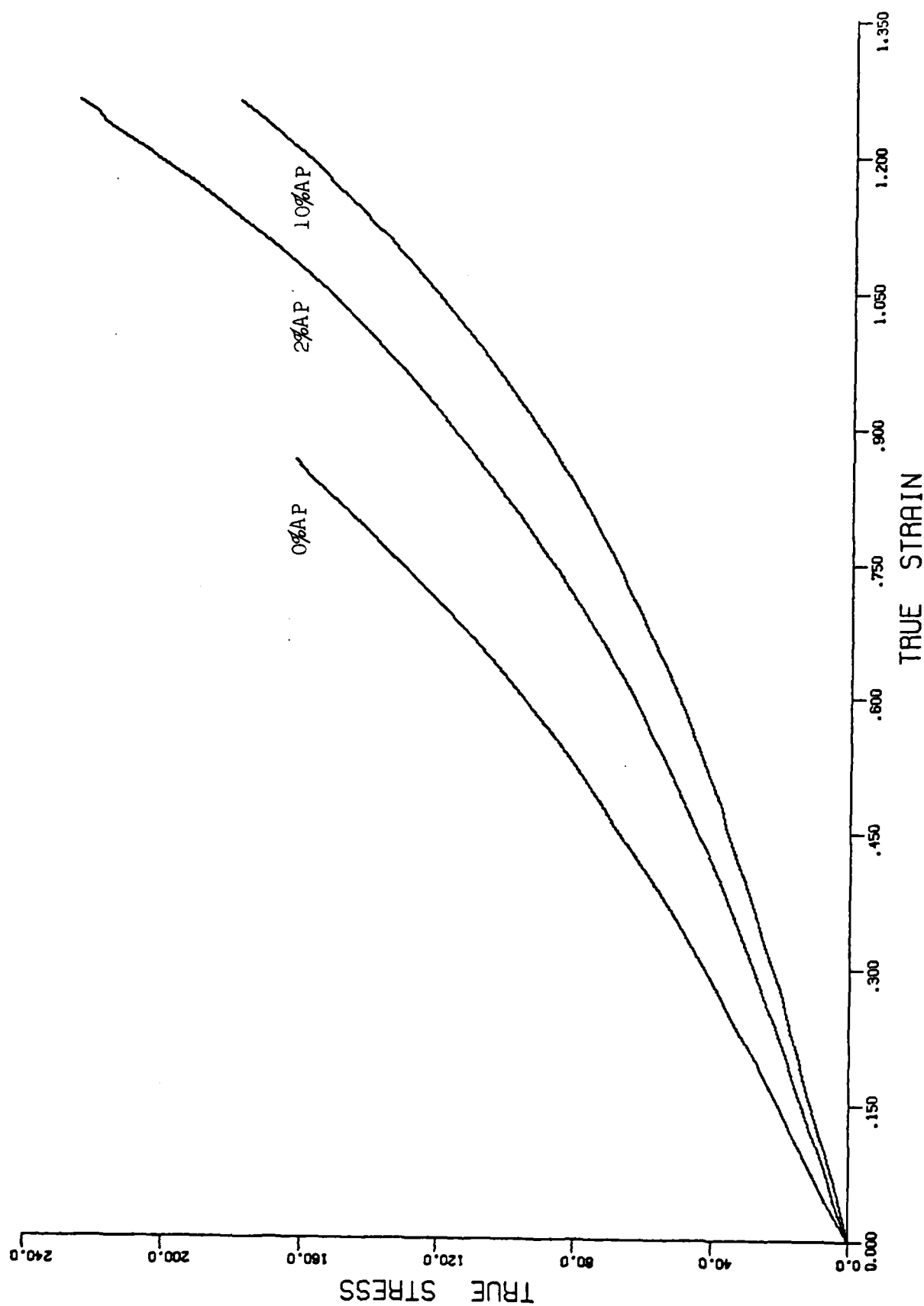
Figure 14. True Stress – True Strain Curves of Propellant Polymer Tested at 1"/"/min
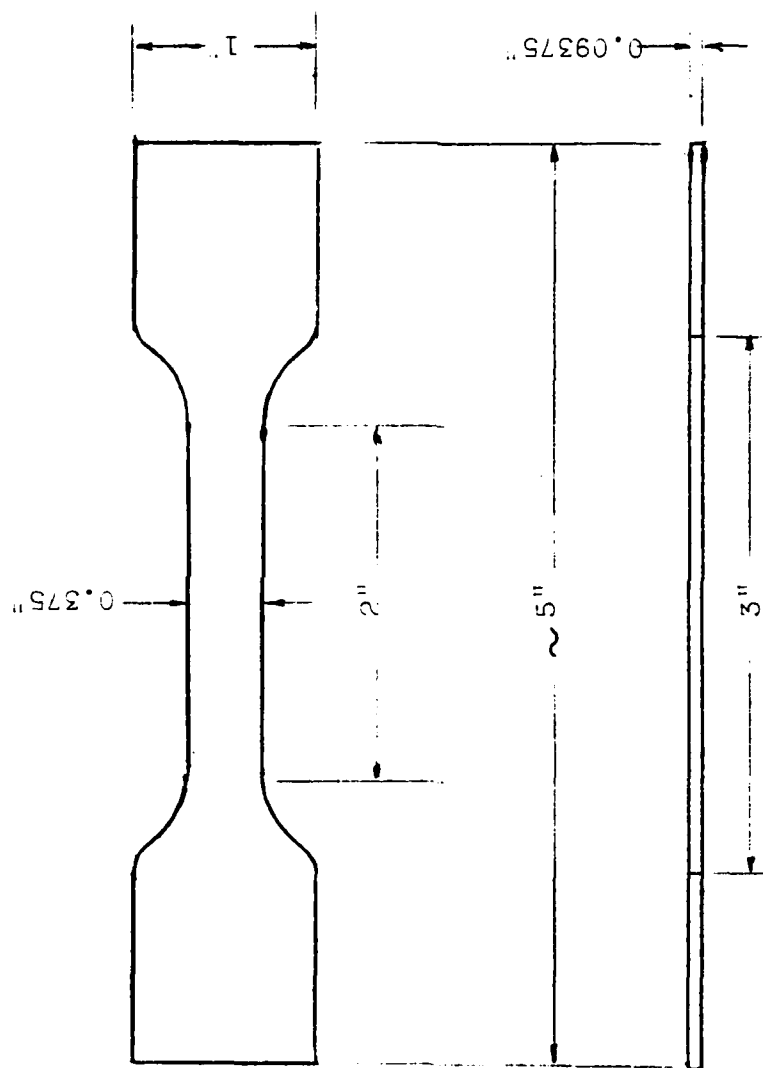
42

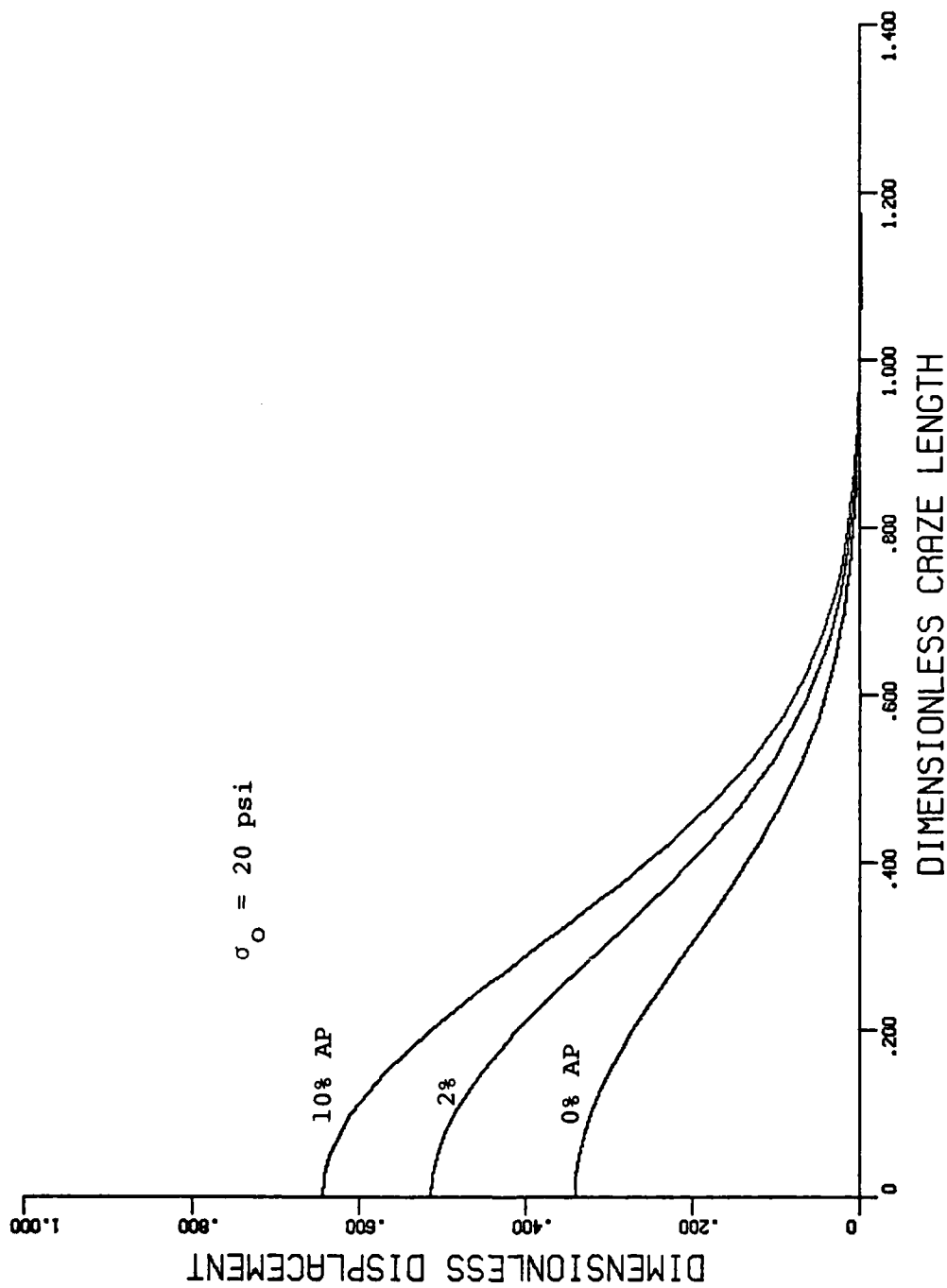Figure 15. Dimensions of Die Cut Propellant Polymer Specimen

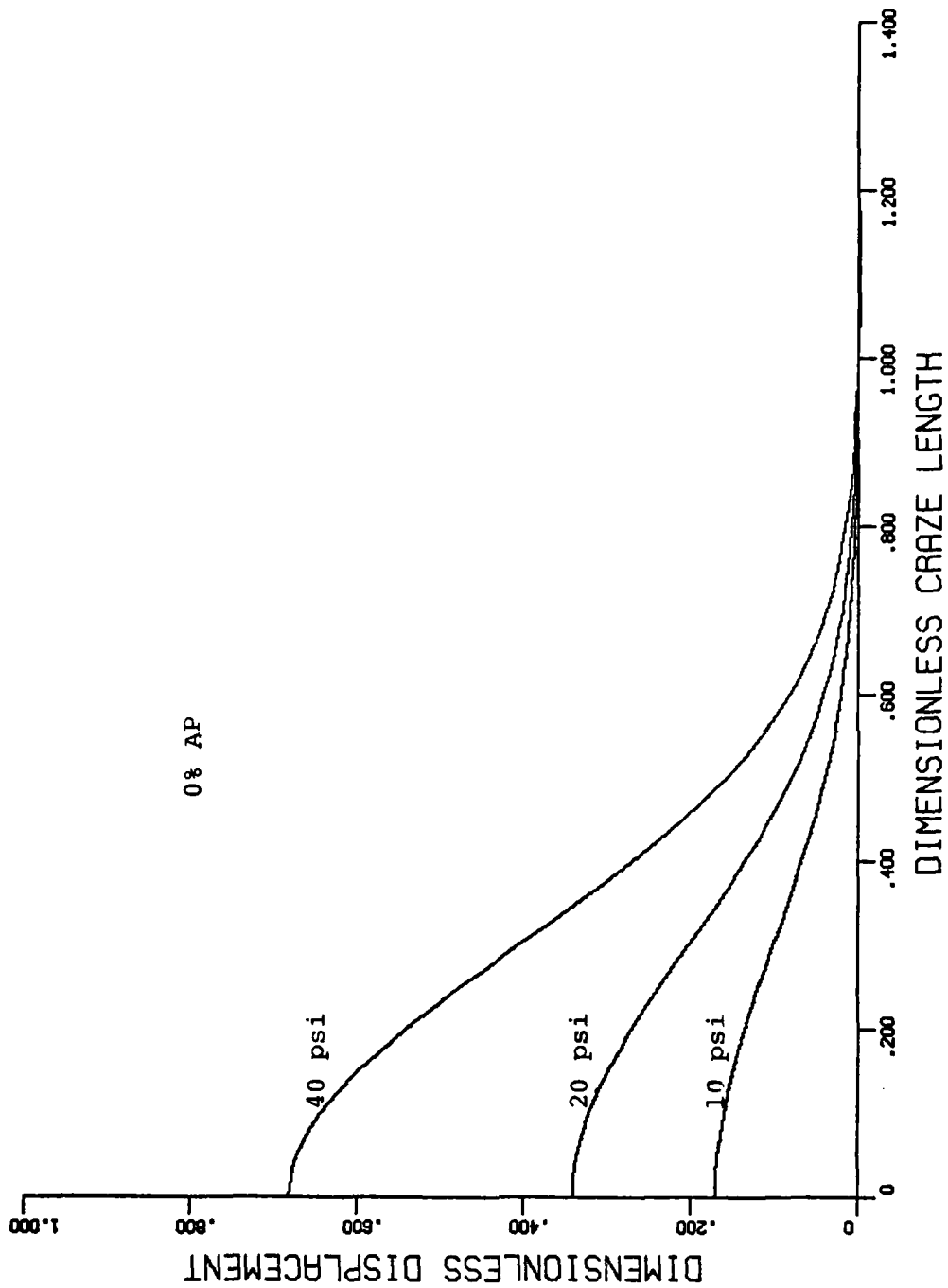Figure 16. Craze Length vs. Craze Displacement at σ_o = 20 psi

44

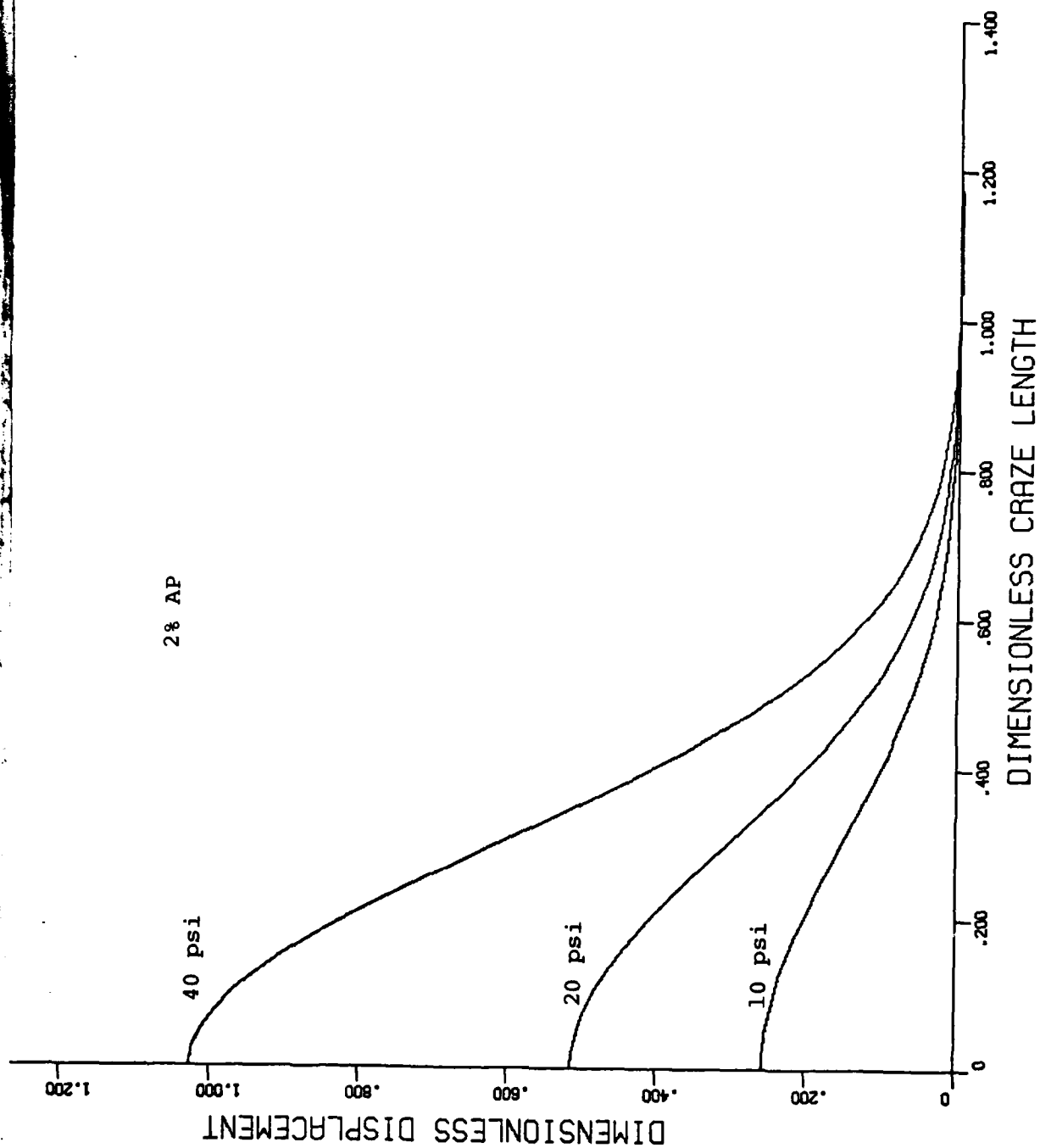Figure 17. Craze Length vs. Craze Displacement at Different Stress Levels

45

Figure 18. Craze Length vs. Craze Displacement at Different Stresses
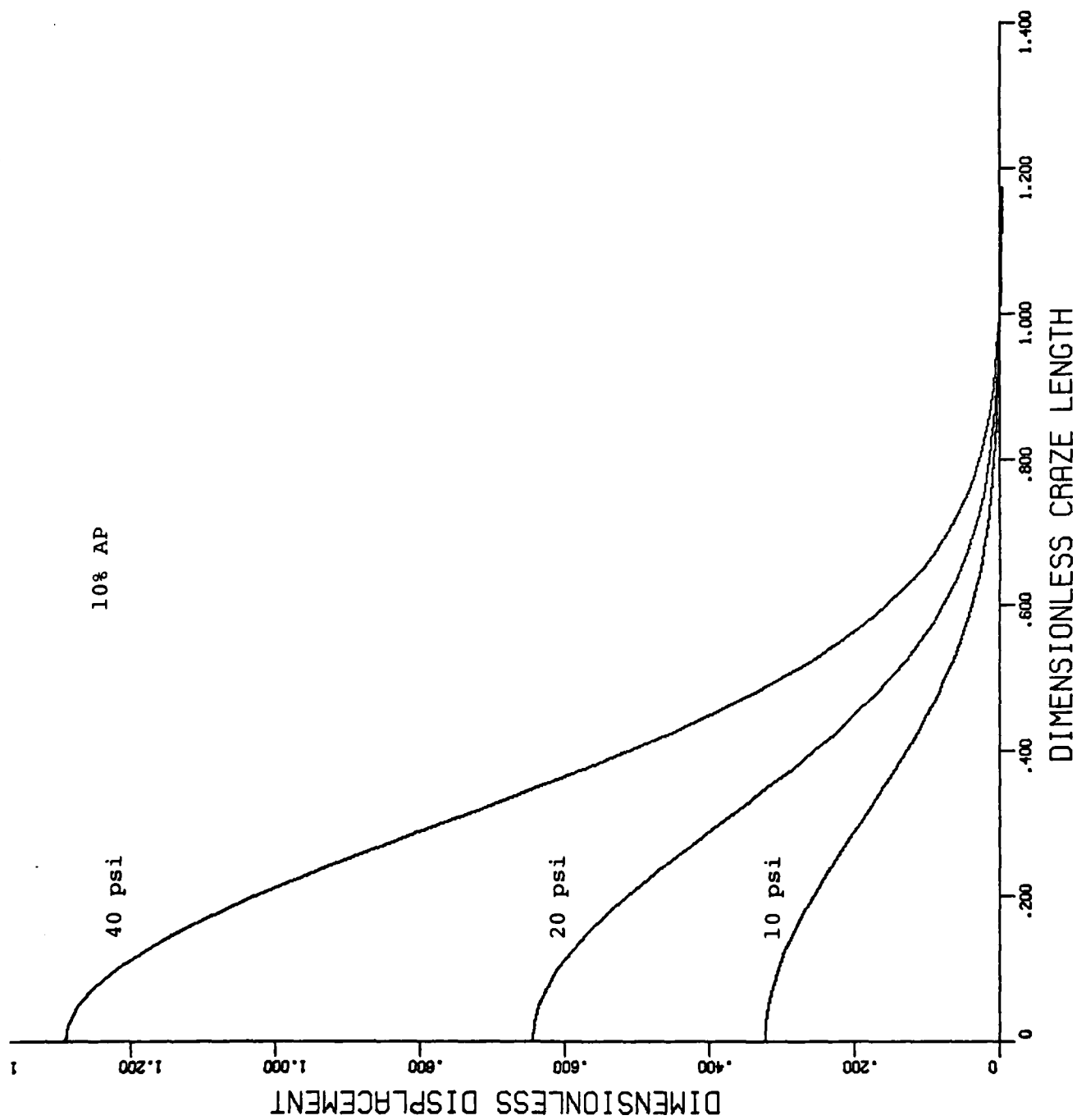
46

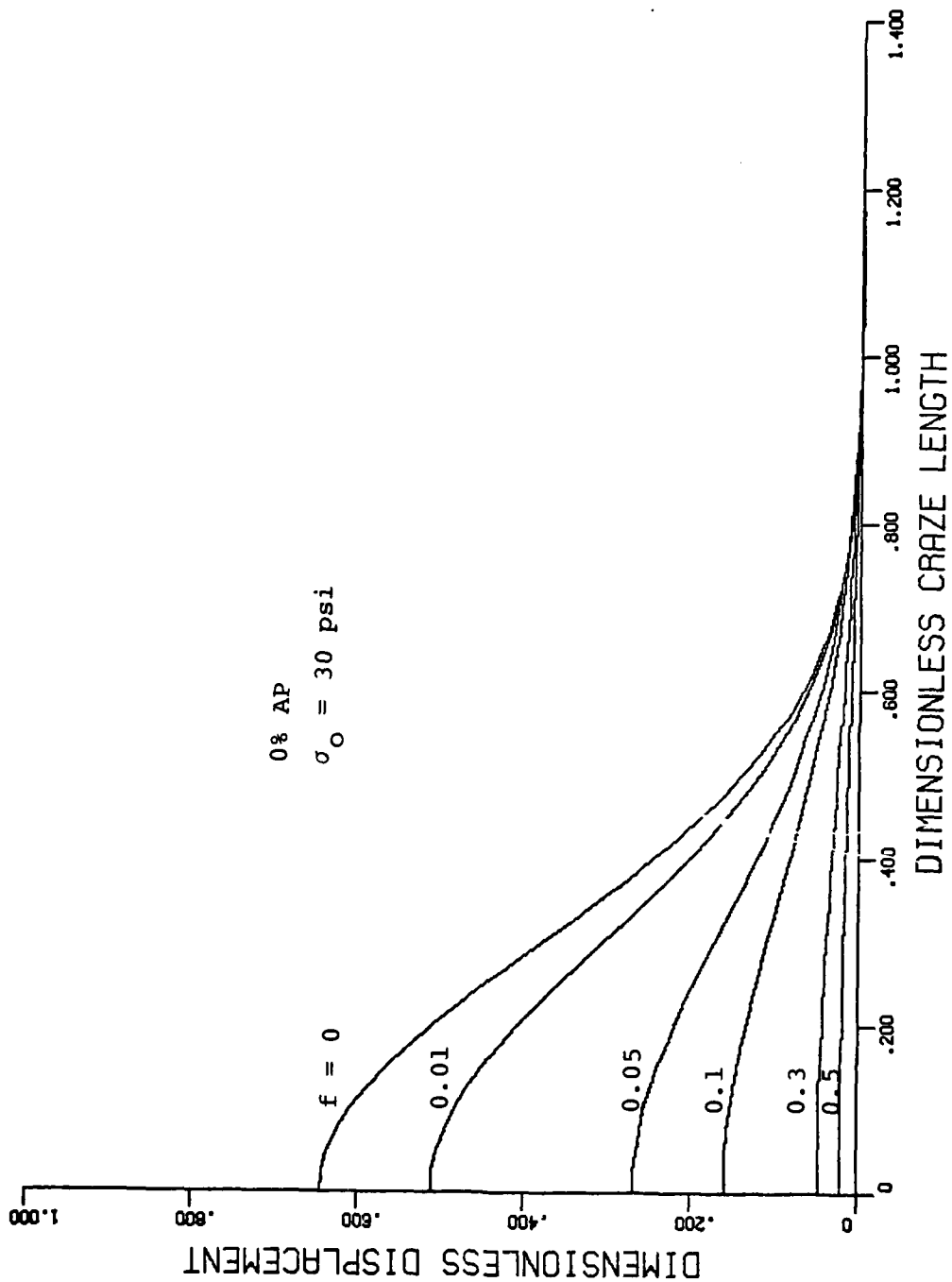Figure 19. Craze Length vs. Craze Displacement at Different Stresses

47

Figure 20. Craze Length vs. Craze Displacement for Different Fractional Strengths at Central Section of Craze.
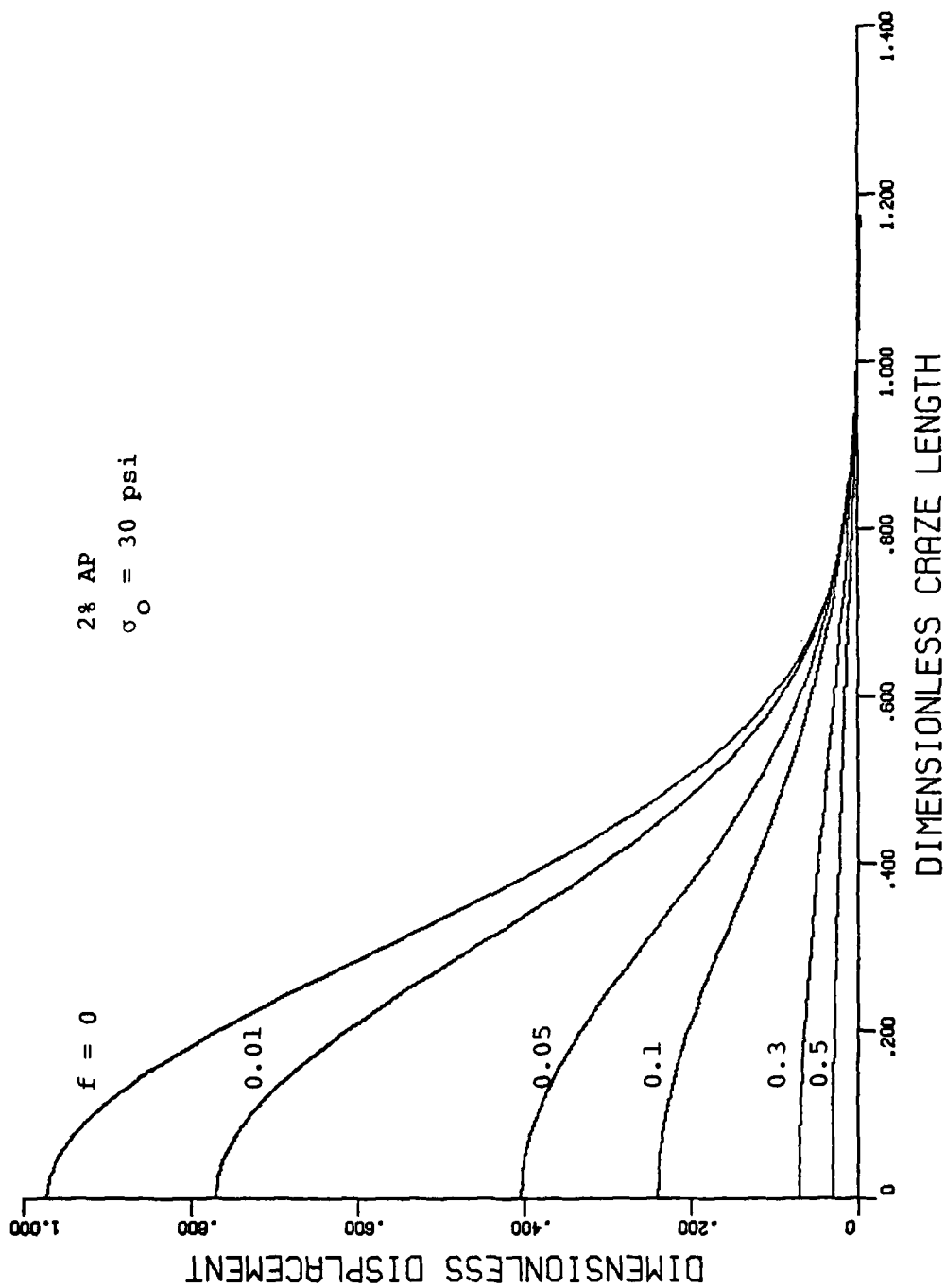
48

Figure 21. Craze Length vs. Craze Displacement for Different Fractional Strengths at Central Section of Craze.
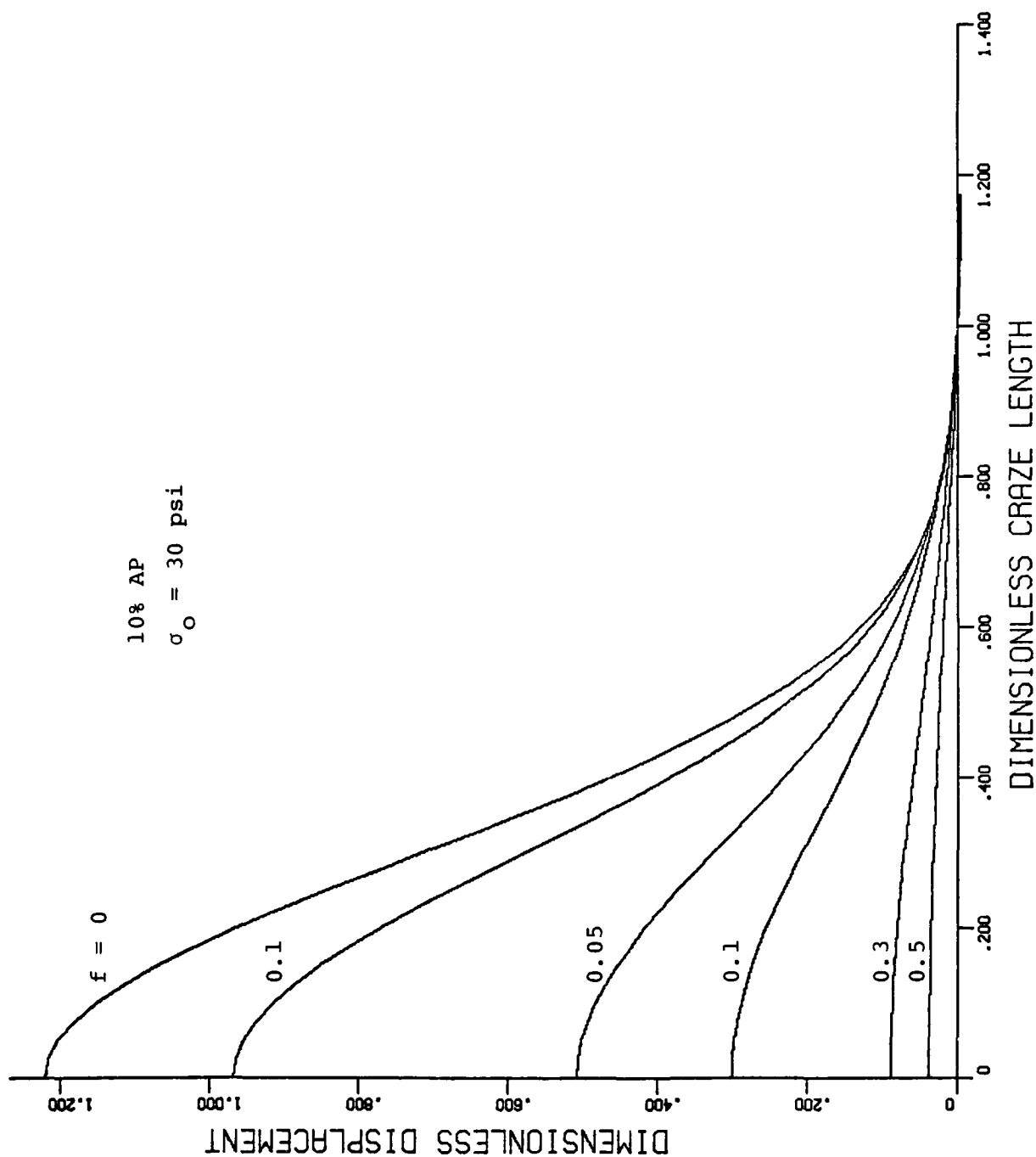
49

Figure 22. Craze Length vs. Craze Displacement for Different Fractional Strengths at Central Section of Craze.

50

by slicing with a sharp blade initially. Afterwards the big craze did grow itself under greater load. It is not known, however, why numerous crazes developed on this specimen and some others while many others did not show any tendency of crazing.

The general agreement between theoretical and experimental results is interesting. It is even more interesting to note that the experimental data only fit those curves in displacements for f = 0.1. Apparently this indicates that the craze material at the central section has reduced to only one tenth of that of the original polymer composites.

As for the stress distribution as affected by different fractional strengths at the central section of the craze, Figure 23 shows the general trend predicted according to the present model.

An actual photomicrograph was taken of a craze as shown in Figure 24. The craze was developed at σ_o = 18.2 psi for a specimen containing 2% ammonium perchlorate. A comparison of theoretical and experimental results is shown in Figure 25. The circles are measured points which agree very well with the theoretical curve with f + 0.1. Under a greater stress, i.e. σ_o = 57.7 psi the displacement field follows the same curve for f = 0.1 as shown in Figure 26.*

2.7 Fracture Initiation and Propagation in Craze Developed in Filled Elastomers

2.7.1 Introduction and Method of Approach - The time-dependent mechanical behavior of highly filled elastomers has received extensive study because of their use as rocket propellants. The filler is typically an inorganic powder with particle diameters within the range of 1 - 200 μ. Filler concentrations as high as 75 - 88% by weight are usually employed. The response of such a

---

* It should be noted here that the flaw depicted in Figure 24 was asymmetrical. The left side of the flaw (i.e. the part not shown in Figure 24) is approximately ¼ the length of the side used in the comparison shown in Figure 25. The maximum opening is (of course) the same for both sides of the flaw in terms of absolute dimensions (Comment added by Air Force Project Manager).
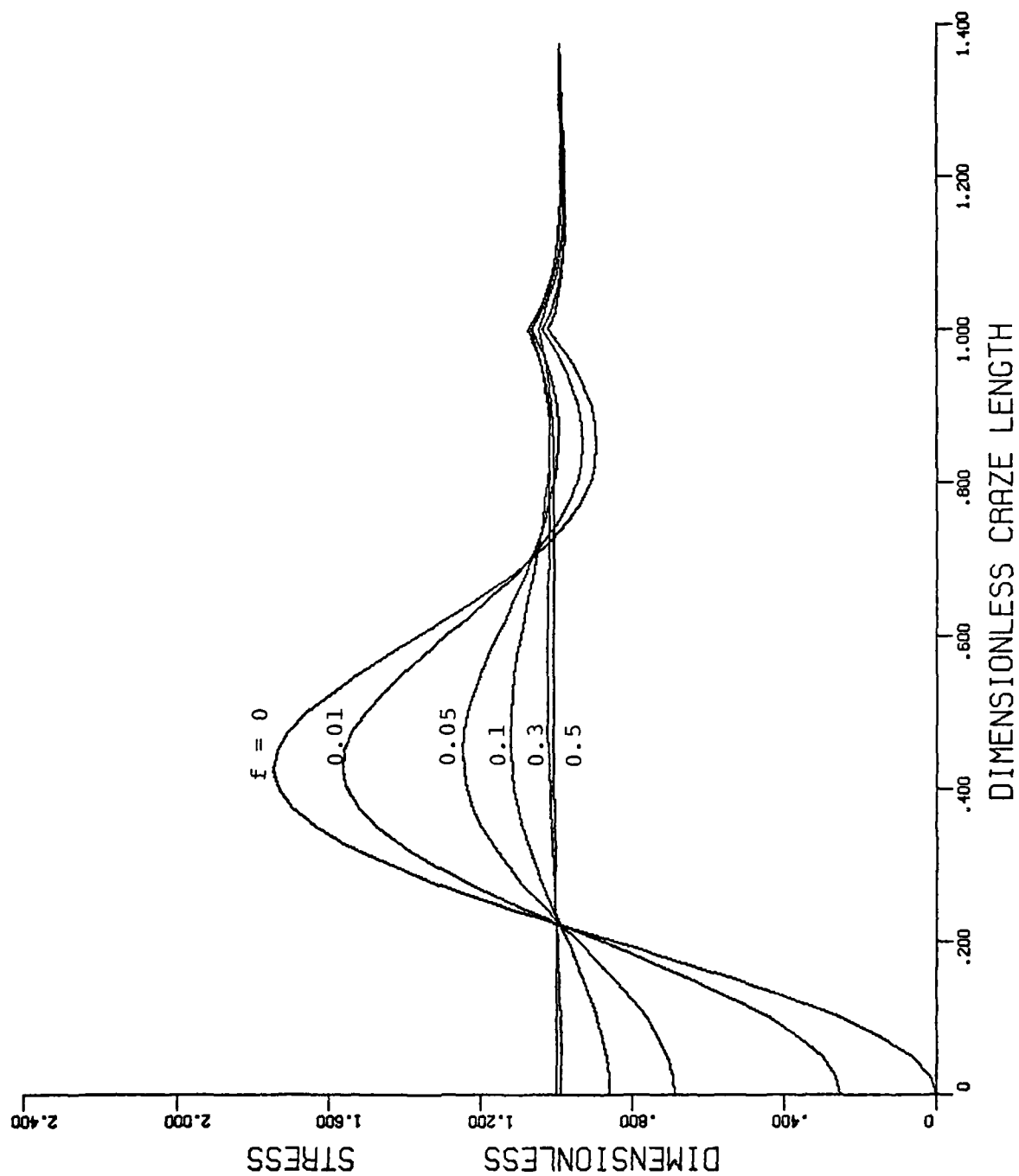
DIMENSIONLESS CRAZE LENGTH

STRESS

DIMENSIONLESS

f = 0
0.01
0.05
0.1
0.3
0.5

0   .200   .400   .600   .800   1.000   1.200   1.400

0   .400   .800   1.200   1.600   2.000   2.400

Figure 23. Craze Length vs. Stress Distribution for Different Fractional
Strengths at Central Section of Craze

52

Figure 24. Craze of Propellant Polymer with 2% Ammonium perchlorate under a Vertical stress of 18.2 psi
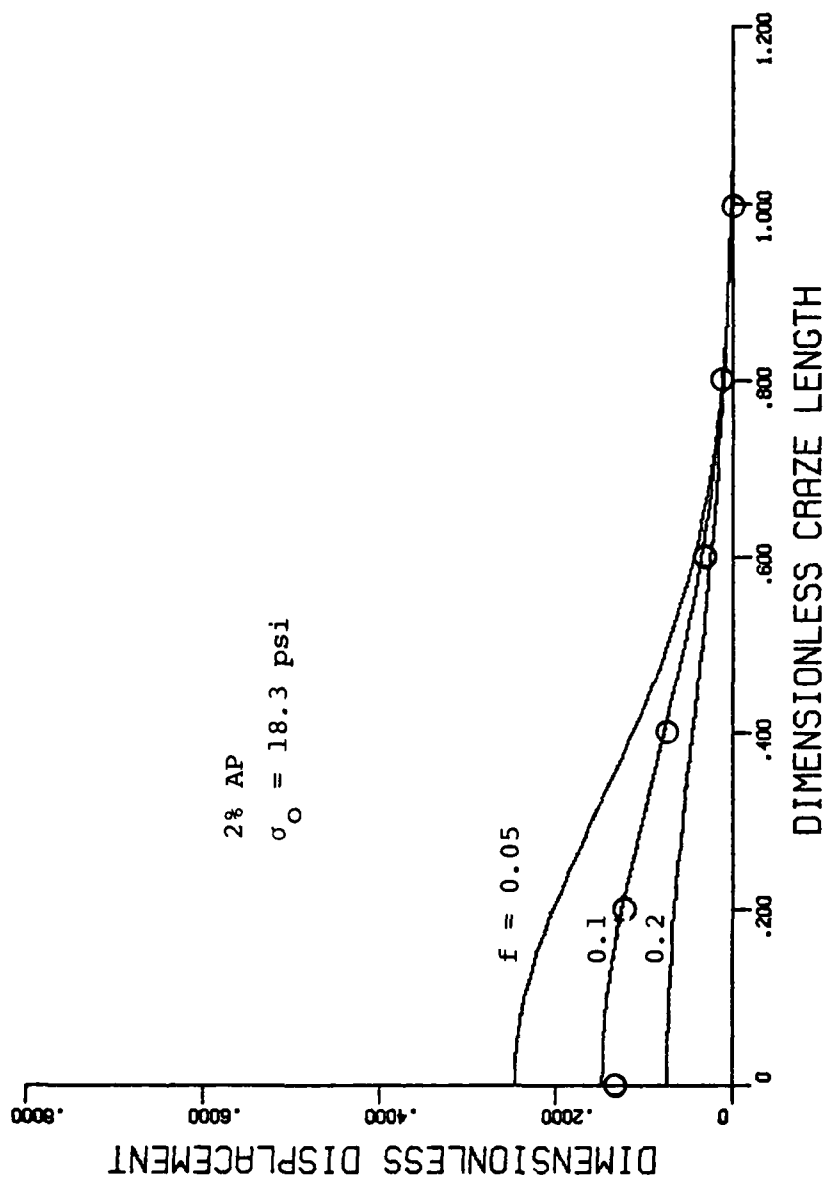
53

Figure 25. Craze Length vs. Craze Displacement for Different Fractional
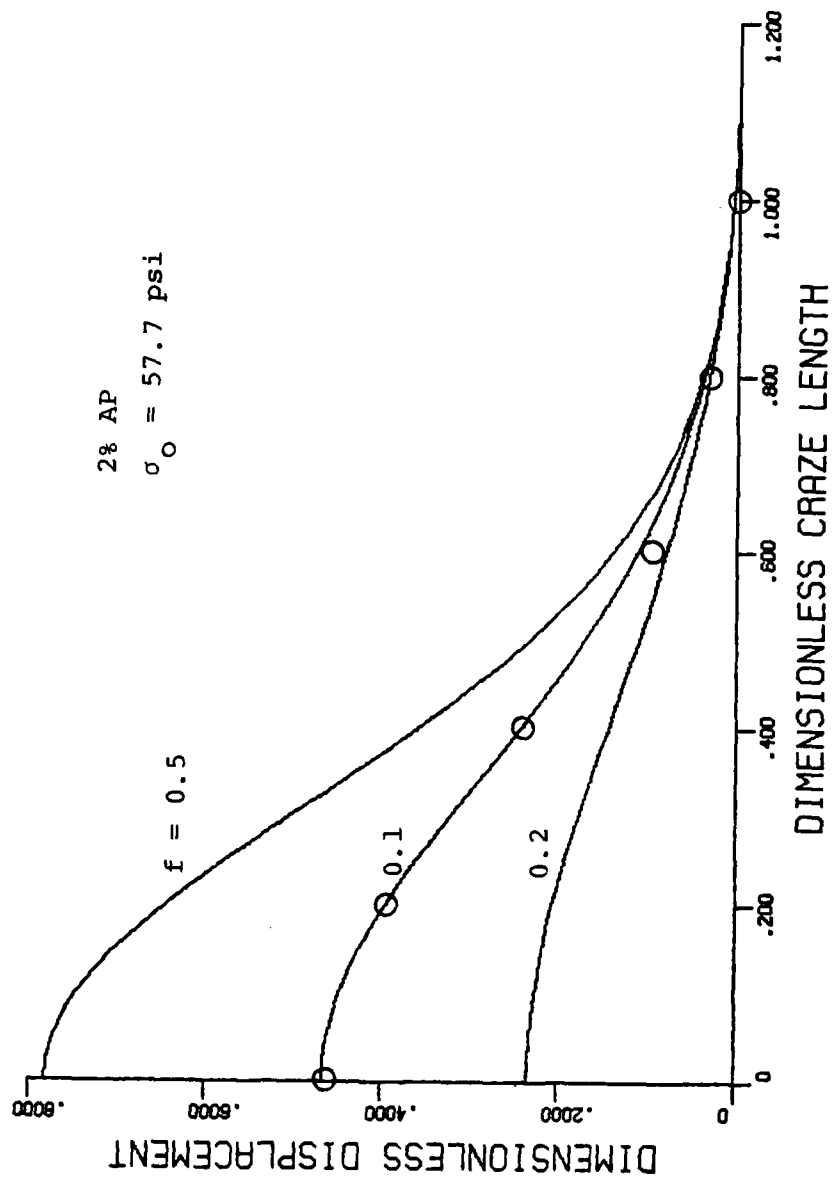Strengths at Central Section of Craze

Figure 26. Craze Length vs. Craze Displacement for Different Fractional Strengths at Central Section of Craze.

material to an imposed stress quite often differs substantially from that of the unfilled elastomer as a consequence of both the reinforcing (or perhaps weakening) action of the filler particle and the surface interactions between the filler and the polymer. For example, the effects of ammonium perchlorate on the stress-strain response and some typical physical properties are shown in Figure 27 and Table 1. These results show that an increase in the percentage of ammonium perchlorate decreases the modulus of elasticity instead of reinforcing it.

One of the most serious and still unresolved problems in high filled solid propellant is the fracture and prefracture behavior of such a polymeric system under load. Why and when do the actual cracks initiate and propagate?

In this report a fracture initiation and propagation mechanism for such polymer system is suggested:

In the neighborhood of particle surfaces, voids initiate due to the breakage of bonds between the filler and the elastomer. They initiate preferentially near large particles or at sites having imperfect bonding.

The breaking of bonds between the filler and the matrix weakens or softens the material such that a localized large strain is generated.

The localized large strains continue to extend until the ultimate strength of the medium is reached.

Finally, the fibrils (rubbery binder) which connect the bulk polymer matrix break down and true fracture initiates.

It appears that the craze fibril bundles play an important role in fracture initiation and propagation. As a result both the nonlinear characteristics of the craze fibrils and their orientation seem to dominate the time dependent mechanical behavior.

Based on these mechanisms, a one-dimensional augmented double beam model (16) together with the reaction rate theory is employed to analyze the time dependent displacement and stress distribution along a craze profile. Figure 28 shows the schematic disgram of the model. A series of springs which connect between two beams are used to represent the craze fibril bundles. Two time dependent quantites $f(t)$ and $\lambda(t)$ are used to measure rupture and

16.   S. S. Chern and C. C. Hsiao, "Prefracture Behavior of Polymer Systems", Section 2.5 in this report (1980).
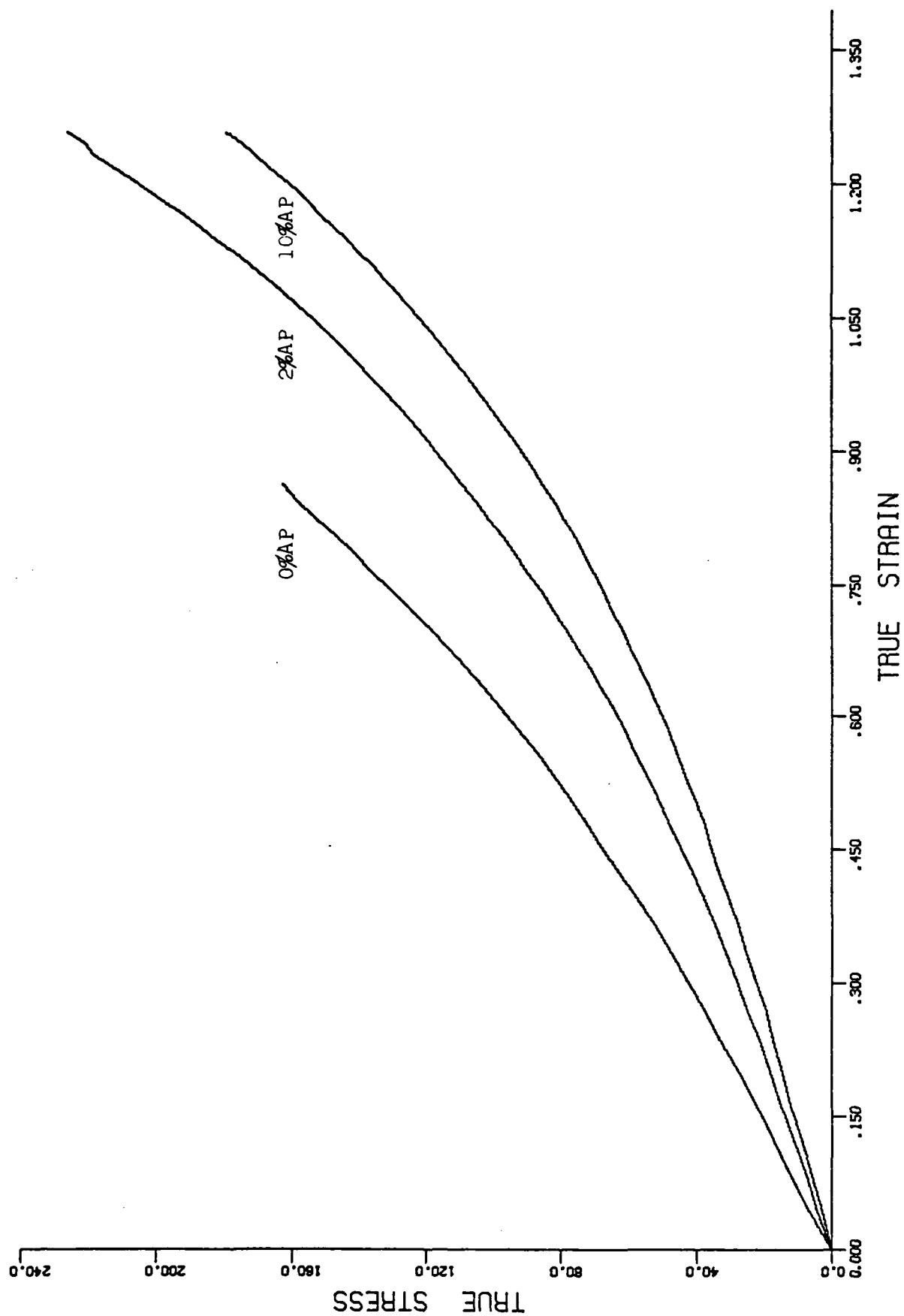
56

Figure 27. True Stress – True Strain Curves of Propellant Polymer Tested at 1"/"/min

57

Table 1. Some Typical Properties of Propellant Polymers

	Units	0% AP	2% AP	10% AP
Engineering Tensile Strength	psi	64	50	46
True Tensile Strength		158	146	175.3
Tensile Elongation		2.47	2.925	3.81
Engineerign Strain	at break*	1.47	1.925	2.91
True Strain		0.9	1.073	1.31
Uniaxial Young's modulus (True Stress - True Strain Curve)	psi	142	94.2	75
Density				

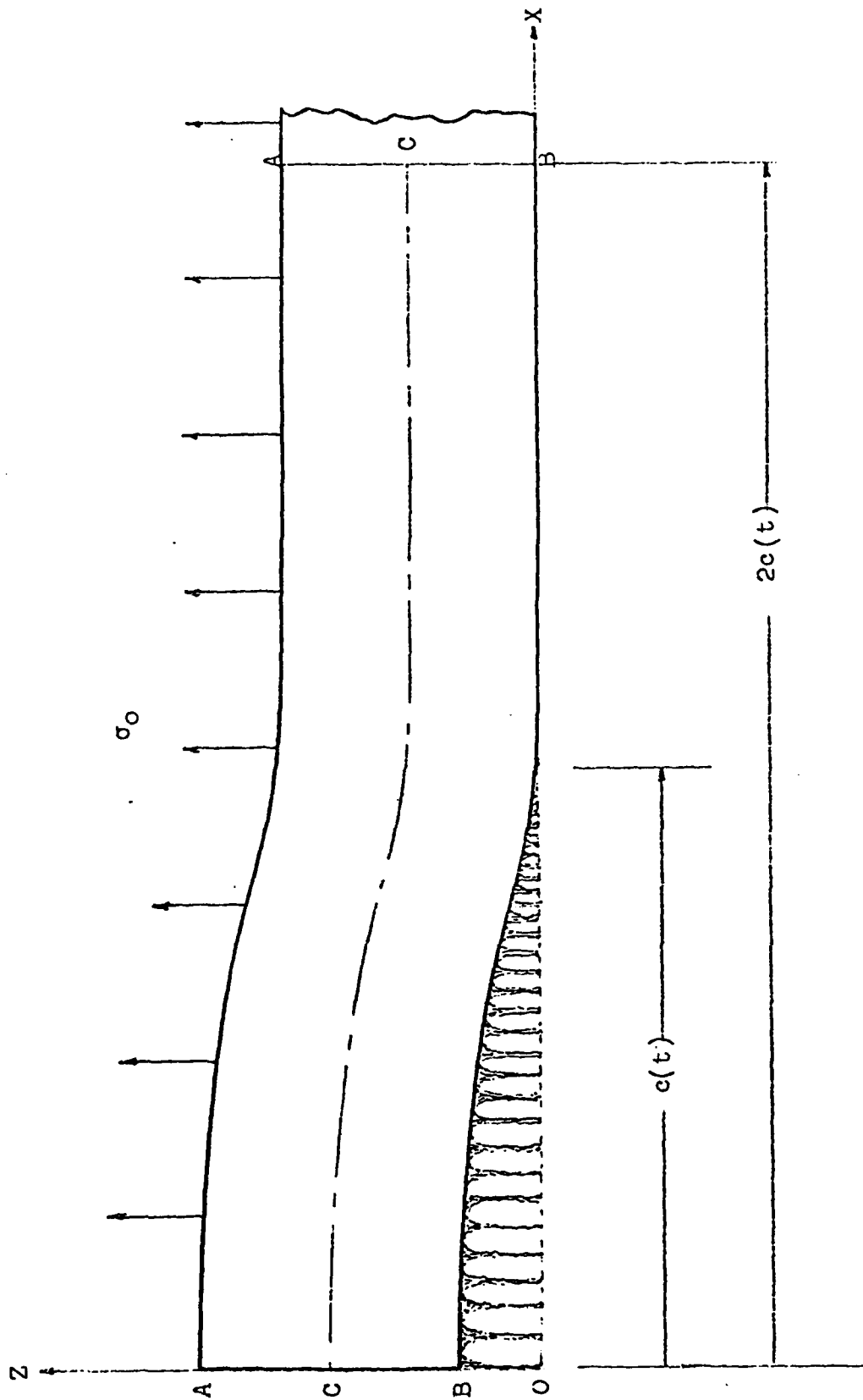* Measured at a Strain rate of 1 in/in/min at 70°F.

Figure 28. Double Augmented Beam Model Showing the Vicinity of a Quadrantal Craze

the orientation of the molecular bonds, respectively. The variation of the ratio of the foundation moduli - that is the modulus with craze present over that without:

$$q[z,f(t),\lambda(t),c(t)] = f(t) + (1 - f(t)) \frac{e^{\lambda(t)z} + e^{-\lambda(t)z} - 2}{e^{\lambda(t)c(t)} + e^{-\lambda(t)c(t)} - 2} \qquad (81)$$

where $f(t)$ is the fraction of unbroken molecular bonds per unit length at the central position of the craze. It is evident that $0 \leq f(t) \leq 1$,

$\lambda(t)$ is a quantity which measures the nonlinearity of the foundation modulus as a result of the orientation of the molecules,

and $c(t)$ is the time dependent craze length measured from the center of a craze. Figure 29 shows several curves on the variation of the foundation modulus q versus the dimensionless craze length $c(t) = 1$, with $f(t) = 0.5$, and $\lambda(t) = 1, 5, 10, 20, 30, 50$.

In general, an excellent approach in obtaining the time dependent behavior has been the use of the statistical theory of the absolute reaction rate (17,18,19) for a system of oriented polymeric molecular elements. Broken elements represent the breakage of molecular bonds under the influence of applied load. This modeling for studying the behavior of craze fibril bundles seems quite adequate as they are oriented molecules. Now let $g(t)$ be the fraction of unbroken elements per unit volume at the central position $x = 0$ of the craze (that is, $f(t) = g^{1/3}(t)$) then the rate of change of g is given as follows:

$$\frac{dg}{dt} = K_r(1 - g) - K_b g \qquad (82)$$

where

$$K_r = \omega_r \exp[-U/RT - \gamma\psi(t)], \qquad (83)$$

$$K_b = \omega_b \exp[U/RT + \beta\psi(t)]. \qquad (84)$$

17. C. C. Hsiao, "Theory of Mechanical Breakdown and Molecular Orientation of a Model Linear High Polymer Solid", J. Appl. Phys., Vol. 30, p. 1492 (1959).
18. C. C. Hsiao, S. R. Moghe and H. H. Kausch von Schmeling, "Time-Dependent Mechanical Strength of Oriented Media", J. Appl. Phys., Vol. 39, 3857 (1968).
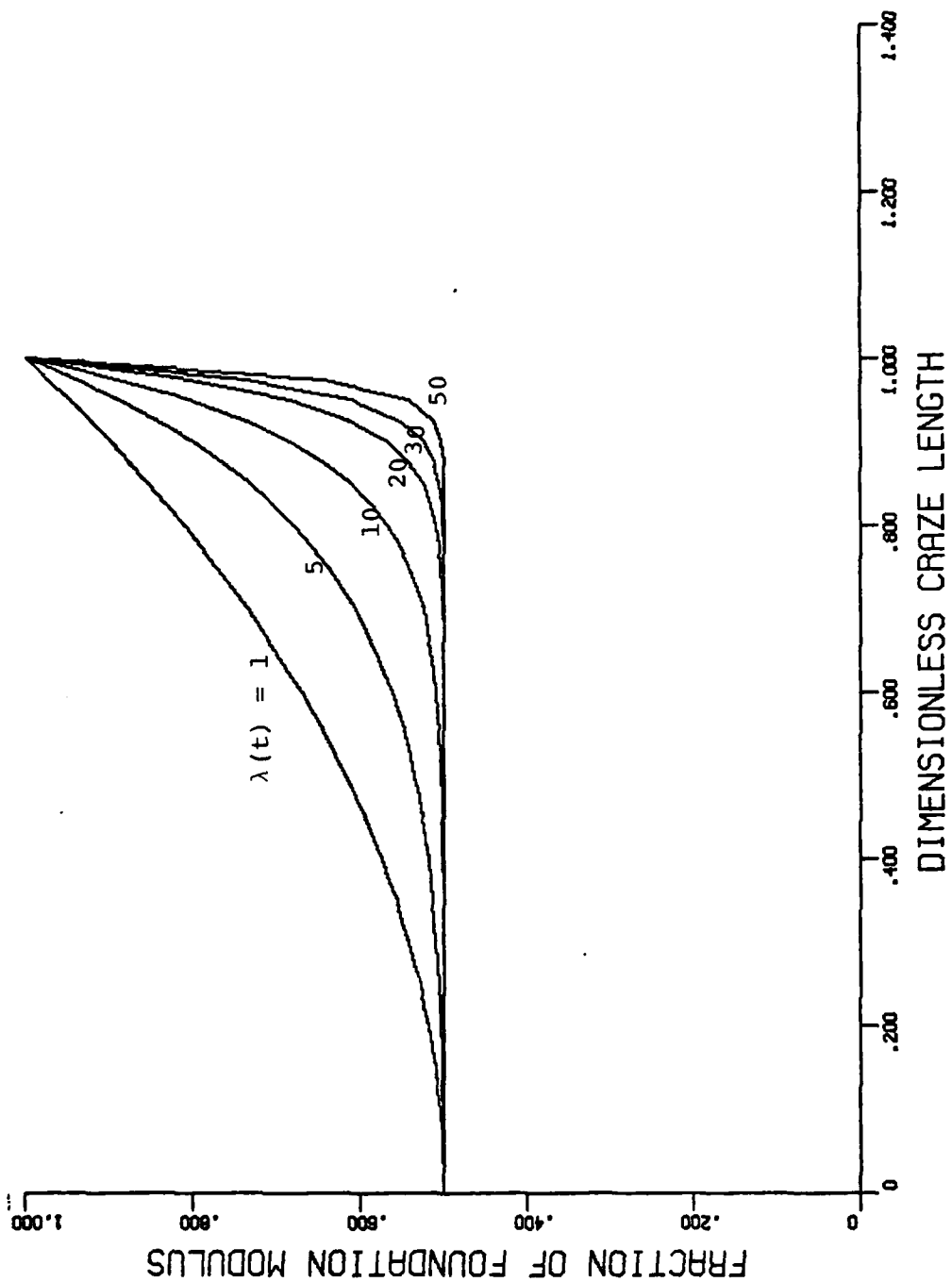19. C. C. Hsiao, "Fracture", Physics Today, Vol 19, 44 (1966).

Figure 29. Craze Length vs. Fraction of Foundation Modulus

61

K_r and K_b are the rate of reformation of broken elements and that of the unbroken elements, respectively. ω_r and ω_b are respectively the frequencies of the jump condition of the elements with respect to the forming and breaking processes,

U is the activation energy,

R is the universal gas constant,

T is the absolute temperature,

γ and β are positive quantities,

$\psi(t)$ is the force per average molecular cross-section in its axial direction.

For moderately large loads (eq. critical crazing load) the influence of reformation can be neglected, that is:

$$K_r = 0. \tag{85}$$

For a uniaxial tension σ_o, $\psi(t)$ is equal to σ_o. Hence K_b is the only material constant left which will govern the function g(t) during rupturing processes. The solution of Equation 82 together with the initial condition that

$$g(0) = g_o, \tag{86}$$

is

$$g(t) = g_o \exp(-K_b t). \tag{87}$$

The value K_b can be determined from experimental creep data under constant loads. It can be shown that β and the term $\omega_b \exp(U/RT)$ are respectively the slope and the intercept of curves plotted with a log of time-to-break versus load.

During the prefracture process, it is reasonable to assume that the craze tip growth mechanism is dominated by steady-state creep. According to a general Arrhenius-type equation, the steady-state craze tip growth velocity can be written as:

$$v = v_0 \exp(-\Delta G / RT) \tag{88}$$

where the quantity v_0 can be thought of as the maximum attainable craze velocity and ΔG as the free enthalpy of activation to overcome one "obstacle". Hence, the time dependent craze length can usually be represented either by

$$c(t) = c_0 + c_1 \ln(t + 1) \tag{89}$$

for the initial stage in creep, or

$$c(t) = c_0 + tv_0 \exp(-\Delta G / RT) \tag{90}$$

for the steady-state creep where c_0 is the initial flaw size from which a craze may develop and c_1 is a constant.

Combining Equations 81, 87 and 89 and some suitably chosen function $\lambda(t)$, the fraction of foundation modulus can be expressed as a time dependent function.

Using this q(t) together with the governing equation and proper boundary condition (Equations 87 and 89) both the time-dependent displacement and stress along the craze profile can be solved.

2.7.2 <u>Stability Criterion of Fracture Initiation and Propagation</u> - A catastrophic failure[*] in a growing craze will occur once critical conditions are reached. Instead of using energy release rate or crack opening displacement (COD) as a critical criterion for crack propagation studies, a volume fraction criterion is proposed:

Let $w_{crack}(x)$ be the displacement field of an elliptical crack in a two-dimensional infinite plane sheet (20).

$$w_{crack}(x) = \frac{2(1-\nu^2) \sigma_0}{E} \sqrt{c^2(t) - x^2} \tag{91}$$

where ν is the Poisson's ratio of bulk polymer and E is its modulus of elasticity.

---

[*] Catastrophic failure refers to a sudden breakdown of craze fibrils.

20. I. N. Sneddon, <u>Fourier Transform</u>, McGraw-Hill, New York, 426 (1951).

Define V_{craze} and V_{crack} as the volumes enclosed by either the craze and crack profile, respectively, that is:

$$V_{craze}(t) = 4 b_o \int_0^{c(t)} w_{craze}(x.t) \, dx, \qquad (92)$$

$$V_{crack}(t) = 4b_o \int_0^{c(t)} w_{crack}(x) \, dx = \frac{2\pi(1-\nu^2)\sigma_o b_o c^2(t)}{E_o}. \qquad (93)$$

Let $G(t) = V_{craze}(t)/V_{crack}(t)$. $\qquad (94)$

Assume that a critical value G_c exists such that when

$G < G_c$: craze is stable

$G \geq G_c$: craze fibrils break down catastrophically

The time t_c such that $G(t_c) = G_c$ is called the fracture initiation time, at which a crack commences and propagates within the craze.

2.7.3 <u>Results</u> - Based upon these ideas, a number of time dependent behaviors have been calculated and plotted.

Under uniaxial tension $\sigma_o = 7.5$ psi for 10% ammonium perchlorate ($E_o = 75$ psi) with initial flaw size $c_o = 0.2$ mm and initial fraction of unbroken bonds $g_o = 0.9$, each elapsed time is considered to be of 5, 10, 20, 30, 40 or 50 minutes, and the other data used are $K_b = 0.1$, $\lambda(t) = 3$, $c(t) = 0.2 + 0.2 \ln(1 + t)$, several plots are given:

Figure 30 shows the time dependent craze displacements.

Figure 31 shows the corresponding time dependent stress distributions along the craze boundary.

Figure 32 shows the corresponding time dependent volume fraction $G(t)$.

Furthermore Figure 33 shows the dependence of the volume fraction $G(t)$ on K_b and $c(t)$.

Similarly with all the quantities the same as given before except that $c(t)$ is chosen to be $0.2 + 0.02$ t, several more illustrations are obtained:

Figures 34 - 36 show plots similar to those of Figures 30 - 32.

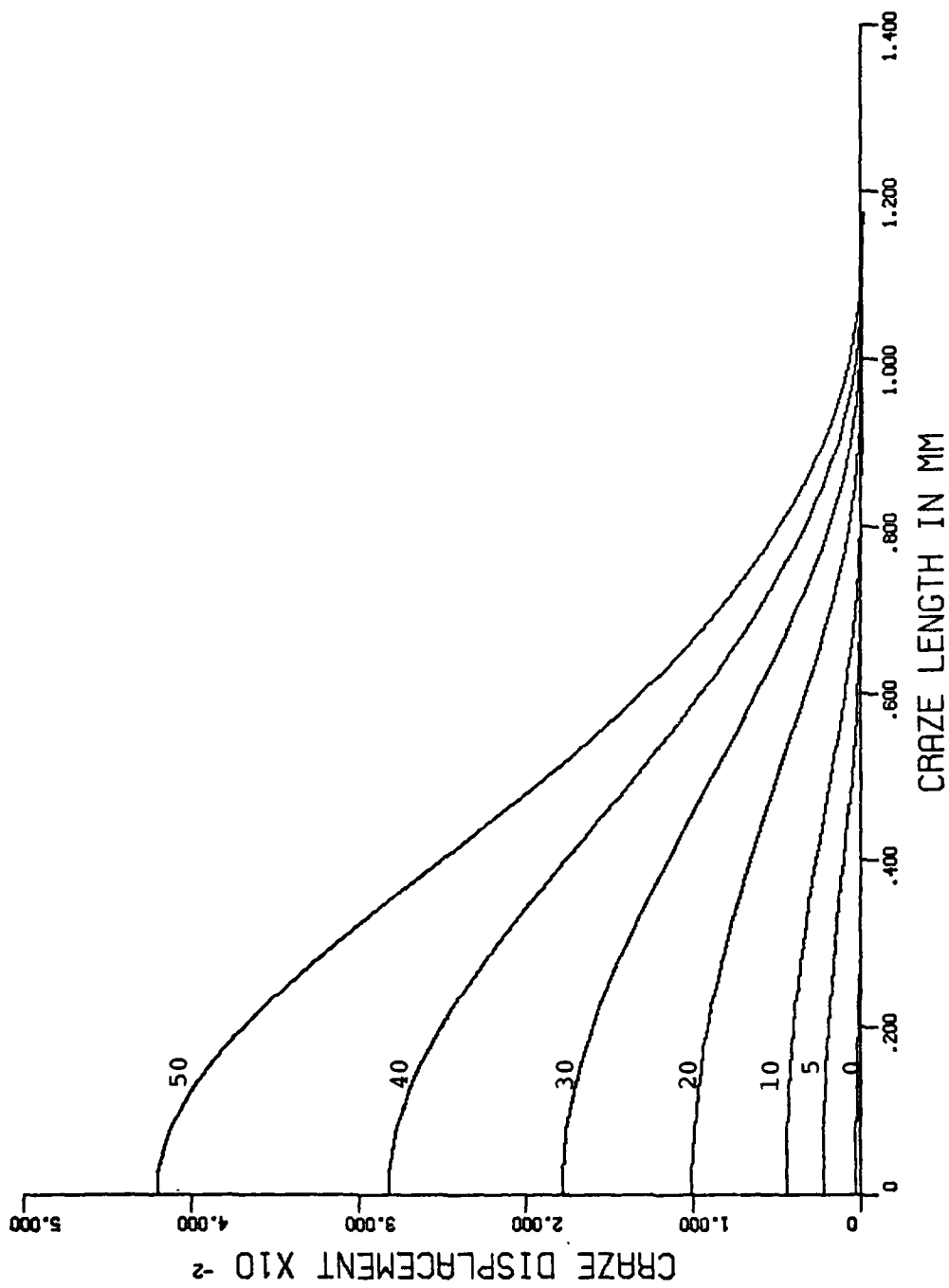In addition Figure 37 shows the dependence of the volume fraction $G(t)$ on K_b and $c(t)$.
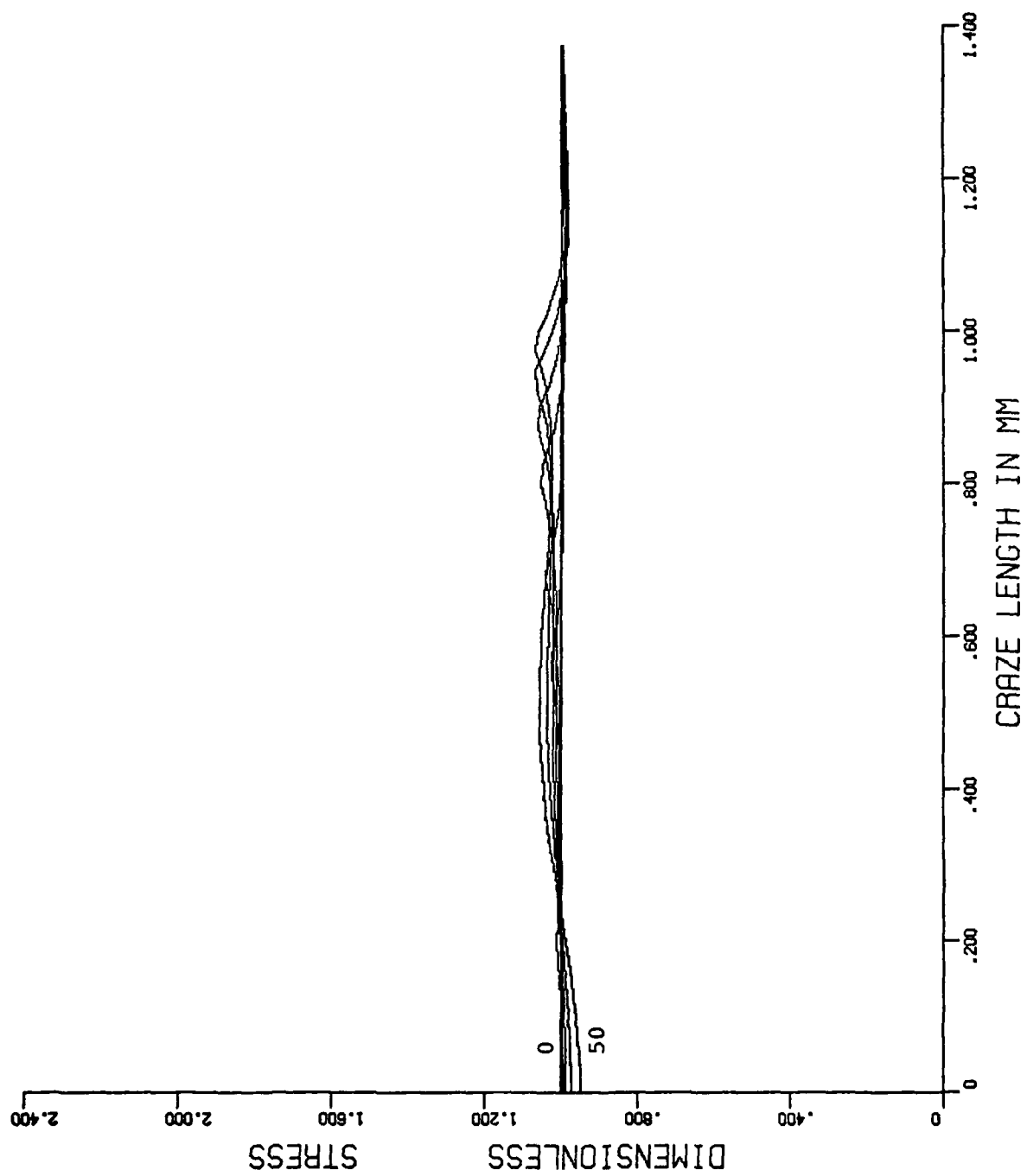
64

Figure 30. Craze Length vs. Craze Displacement

Figure 31. Craze Length vs. Stress Distribution

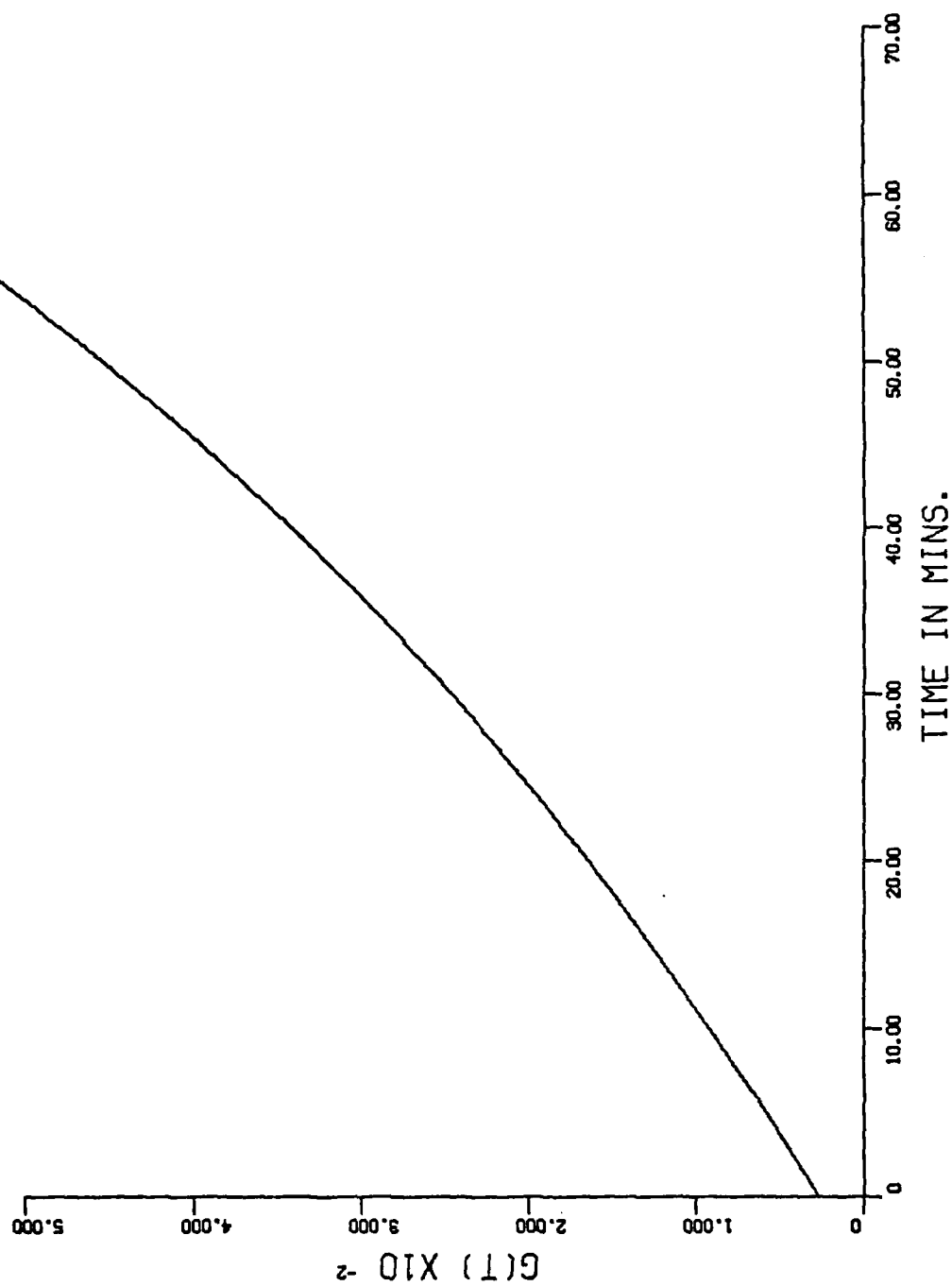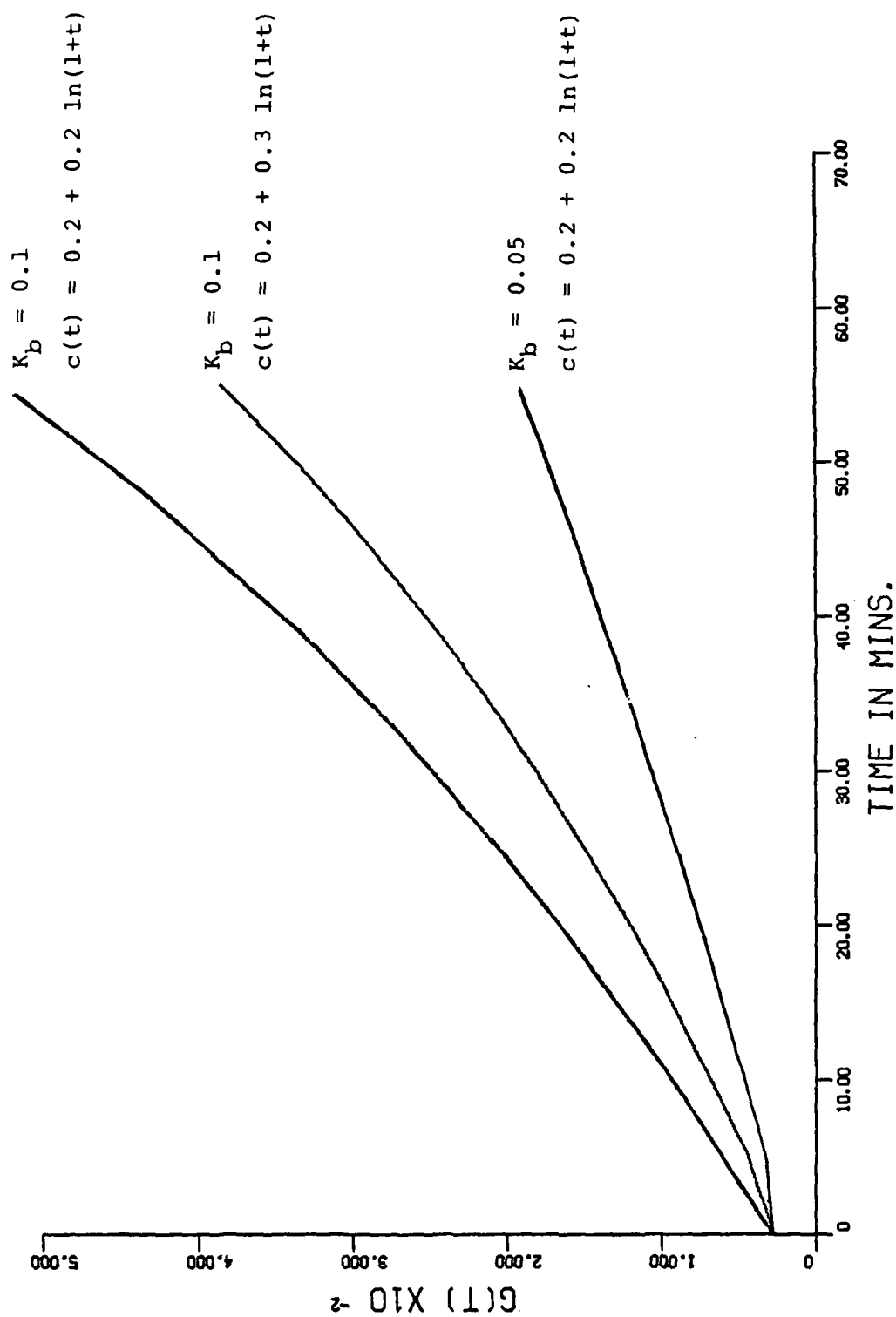Figure 32. Time vs. Volume Fraction G(t)
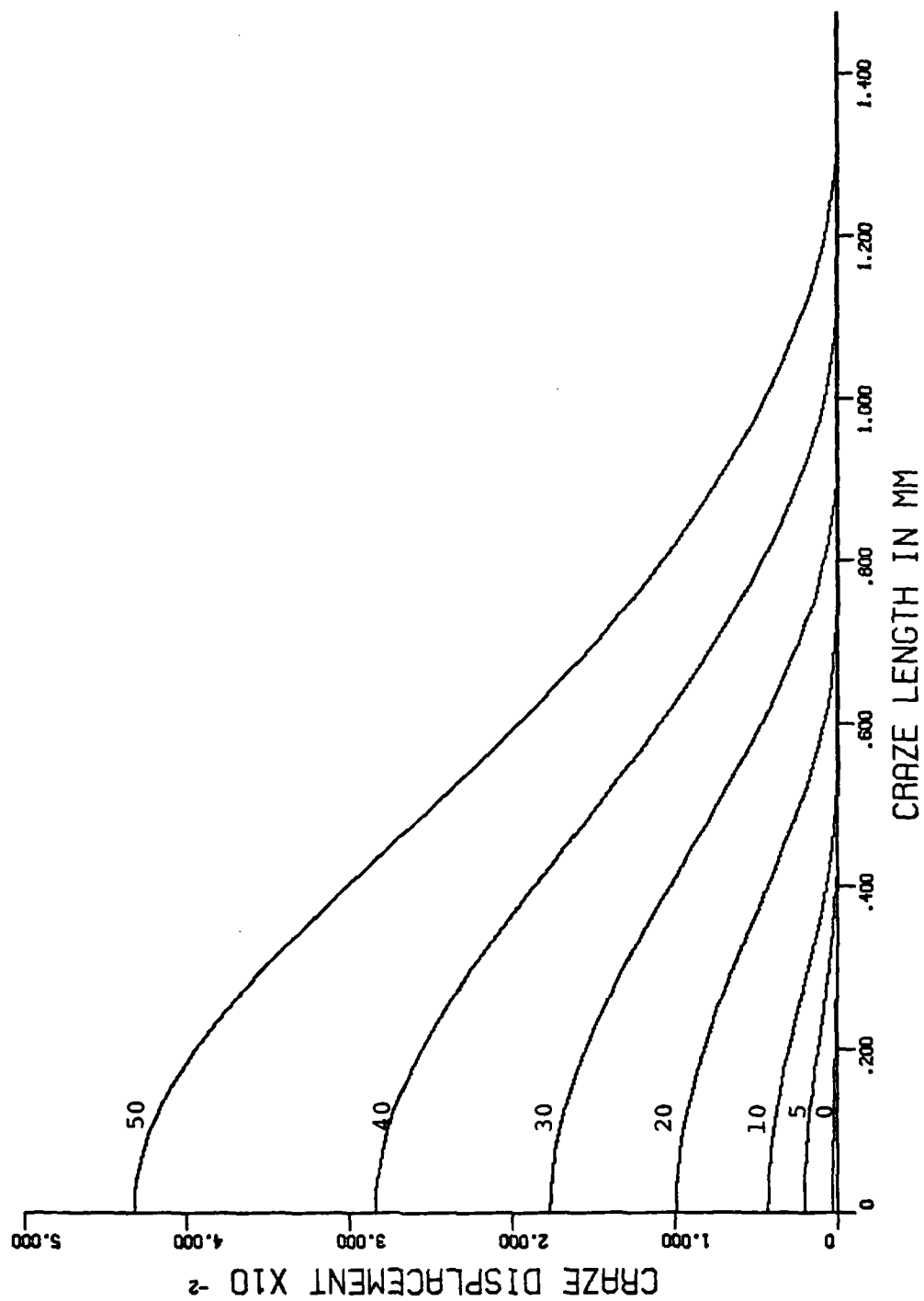
Figure 33. Time vs. Volume Fraction G(t)

68

Figure 34. Craze Length vs. Craze Displacement
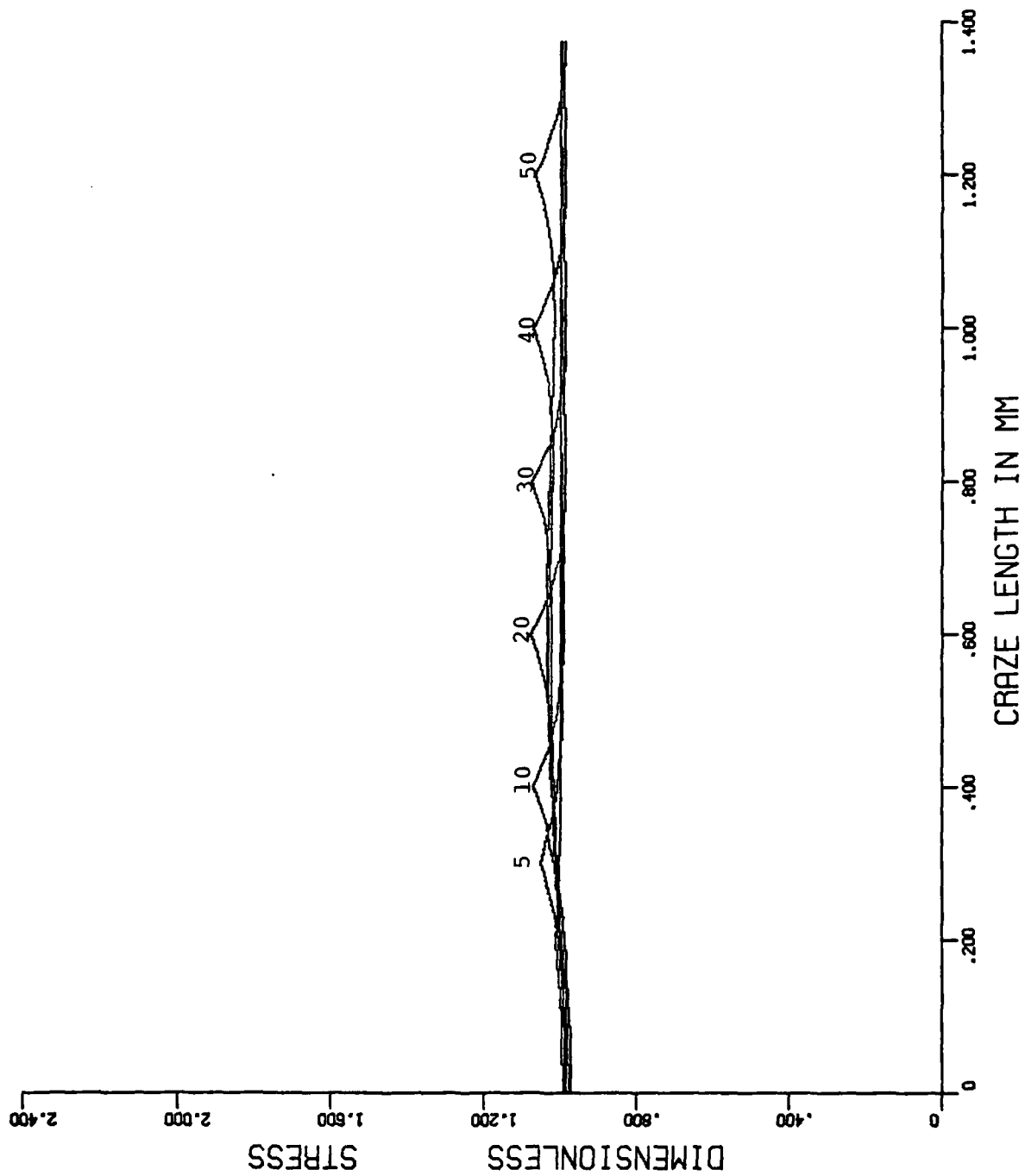
Figure 35. Craze Length vs. Stress Distribution

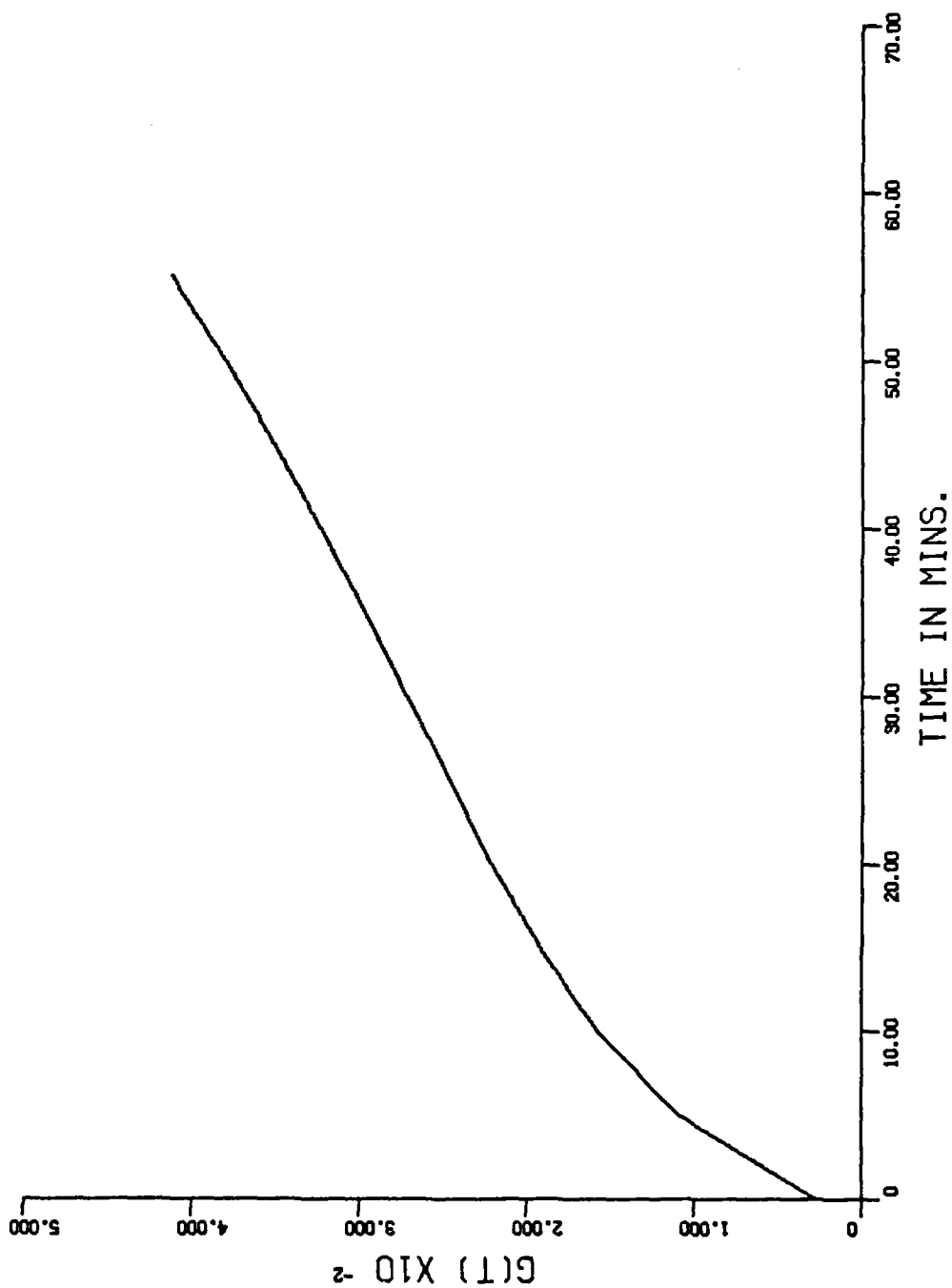Figure 36. Time Dependent Volume Fraction G(t)
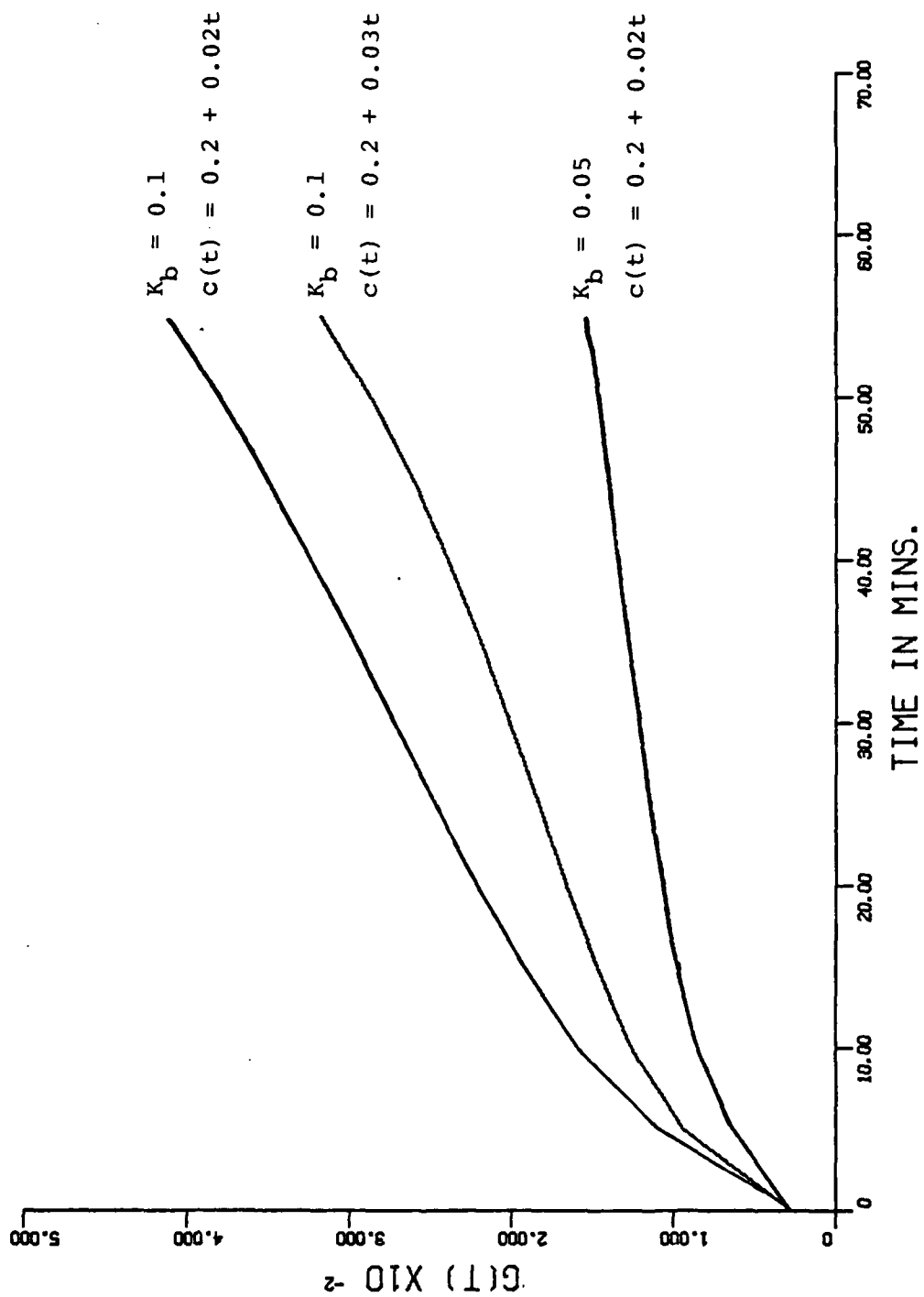
Figure 37. Time vs. Volume Fraction G(t)

The figure shows a plot with the vertical axis labeled "G(T) X10 $^{-2}$" ranging from 0 to 5.000, and the horizontal axis labeled "TIME IN MINS." ranging from 0 to 70.00.

Curves are labeled:

$K_b = 0.1$
$c(t) = 0.2 + 0.02t$

$K_b = 0.1$
$c(t) = 0.2 + 0.03t$

$K_b = 0.05$
$c(t) = 0.2 + 0.02t$

2.7.4 <u>Remarks</u> - Unlike fracture mechanics, where energy release rate is widely used as a fracture criterion, the load-bearing capability of craze fibril bundles makes it difficult to express energy release rate as function of craze tip growth only. In fact, the energy release rate is not only a function of time but also functions of craze length, fibrous strength and breaking rate of fibrils. In this report, the reaction rate theory is employed to calculate the breaking rate of fibrils and the time dependent nonlinear behavior of the foundation modulus. Then an augmented double beam model is used to find the displacement of craze profile and <u>load-bearing capacity</u> of craze fibrils. Finally, a volume fraction is proposed as an instability criterion of the whole craze-crack transition. The results show that the instability behavior of craze is dominated by the breaking rate of craze fibrils instead of the growing velocity of the craze tip.

4. FINAL REMARKS

The complex problem of prefracture of propellant polymer has been successfully tackled. Several possible theoretical developments have been made. Some experimental evidences in support of the mathematical modelings have been found. A new laser speckle interferometric technique for measuring in-plane displacement fields has been successfully developed. This together with the augmented double beam model for craze stress analyses has paved the way to study crazing in solid propellant polymer systems. The basic theory has also been extended to cover a possible investigation on the fracture initiation of propellant polymers. These theories and methods can be tested once proper data associated with propellant polymers become available.